

# Effects of Tidal Shocks on the Evolution of Globular Clusters

Oleg Y. Gnedin

Princeton University Observatory, Princeton, NJ 08544;  
ognedin@astro.princeton.edu

Hyung Mok Lee

Department of Earth Sciences, Pusan University, Pusan 609-735  
and Department of Astronomy, Seoul National University, Seoul 151-742, Korea;  
hmlee@astro.snu.ac.kr

Jeremiah P. Ostriker

Princeton University Observatory, Princeton, NJ 08544;  
jpo@astro.princeton.edu

## ABSTRACT

We present new Fokker-Planck models of the evolution of globular clusters, including gravitational tidal shocks. We extend our calculations beyond the core collapse by adopting three-body binary heating. Effects of the shocks are included by adding the tidal shock diffusion coefficients to the ordinary Fokker-Planck equation: the first order heating term,  $\langle \Delta E \rangle$ , and the second order energy dispersion term,  $\langle \Delta E^2 \rangle$ . As an example, we investigate the evolution of models for the globular cluster NGC 6254. Using the *Hipparcos* proper motions, we are now able to construct orbits of this cluster in the Galaxy. Tidal shocks accelerate significantly both core collapse and the evaporation of the cluster and shorten the destruction time from 24 Gyr to 18 Gyr. We examine various types of adiabatic corrections and find that they are critical for accurate calculation of the evolution. Without adiabatic corrections, the destruction time of the cluster is twice as short.

We examine cluster evolution for a wide range of the concentration and tidal shock parameters, and determine the region of the parameter space where tidal shocks dominate the evolution. We present fitting formulae for the core collapse time and the destruction time, covering all reasonable initial conditions. In the limit of strong shocks, the typical value of the core collapse time decreases from  $10 t_{rh}$  to  $3 t_{rh}$  or less, while the destruction time is just twice that number. The effects of tidal shocks are rapidly self-limiting: as clusters lose mass and become more compact, the importance of the shocks diminishes. This implies that tidal shocks were more important in the past.

*Subject headings:* stellar dynamics — globular clusters: general — globular clusters: individual (NGC 6254)

## 1. Introduction

Evolution of star clusters is driven by a variety of dynamical processes. Two-body relaxation, stellar evolution, evaporation of stars, and tidal truncation have all been shown to play a role. In addition to the internal effects, the external tidal shocks from the Galaxy are very important. Gnedin & Ostriker (1997)

found that tidal shocks contribute at least as much as two-body relaxation to the destruction of the current Galactic sample of globular clusters.  $N$ -body simulations of Gnedin & Ostriker (1999) provide a detailed account of the effect of individual tidal shocks on the stellar energy distribution. In this paper we describe the implementation of tidal shocks in a Fokker-Planck code and present new models of globular cluster evolution.

The study of the dynamical evolution of globular clusters has a long and rich history. Spitzer (1987), Meylan & Heggie (1997), and Ashman & Zepf (1998) provide comprehensive reviews of the evolution of isolated and tidally-limited clusters. Two-body relaxation causes loosely-bound stars gain velocity higher than the escape velocity, which leads to their evaporation from the cluster (Ambartsumian 1938; Spitzer 1940). Even without evaporation, clusters would experience a catastrophic collapse driven by the negative heat capacity and the conductive transport of the thermal energy from the inner to the outer parts of the cluster (Antonov 1962; Lynden-Bell & Wood 1968; Goodman 1987). The run-away process leads to a gravothermal catastrophe, or core collapse. The collapse can be reversed when a sufficient amount of heating is provided in the core via formation of binaries. The successive mergers of normal stars and subsequent supernova explosions were also shown to be effective in halting the collapse (Lee 1987). After the reversal of core collapse, the evolution of the cluster can be characterized by quasi-static expansion with possible gravothermal oscillations.

The tidal field of the Galaxy affects cluster dynamics in two ways. The stellar distribution is effectively cut off at the point where the ambient Galactic density exceeds that of stars in the cluster. Lee & Ostriker (1987) found that clusters with short initial relaxation time dissolve in  $\sim N/200$  orbital periods around the Galaxy, where  $N$  is the initial number of stars in the cluster. Tidal effects may also cause cluster rotation as the stars on prograde orbits have higher chances to be ejected than those on retrograde orbits (e.g., Oh & Lin 1992). In addition, the time-varying tidal forces cause gravitational shocks when the cluster passes through the disk of the Galaxy (Ostriker, Spitzer, & Chevalier 1972) or comes near the Galactic nucleus (e.g., Spitzer 1987). Tidal shocks increase random motion of stars and reduce cluster binding energy. Finally, Kundić & Ostriker (1994) and Gnedin & Ostriker (1997) emphasized that the tidal shock relaxation can be very important in accelerating cluster evolution. Recent studies (Murali & Weinberg 1997a-c; Ostriker & Gnedin 1997) show that these effects can lead to substantial evolution of the globular cluster population.

All of the above processes are included in our Fokker-Planck code. We discuss the detailed implementation of tidal shocks and demonstrate their effects on the evolution of clusters with a wide range of parameters. We consider both single-mass models and models including a spectrum of stellar masses. Mass segregation and rapid energy transfer between the stars of different masses lead to an even faster core collapse and destruction of globular clusters. Although we do not include the effects of stellar evolution, they are likely to be important only at the early stages of cluster evolution. Chernoff & Shapiro (1987) and Chernoff & Weinberg (1990) showed that the mass loss from the short-lived massive stars can disrupt weakly concentrated clusters (with  $c \lesssim 0.6$ ). We also ignore the effects of rotation and velocity anisotropy but discuss the latter at the end of the paper.

We first review the theory of tidal shocks in §2. The new features of the Fokker-Planck code are described in §3. We start with an illustrative case that demonstrates the importance of tidal shocks and adiabatic corrections in §4. More systematic study for a wide range of the parameter space is presented in §5. Finally, we discuss the implications of our results to the evolution of the Galactic star clusters.

## 2. Review of the Theory of Tidal Shocks

The first and second order theory of the compressive (disk) shocks and tidal (bulge) shocks has been developed by Ostriker, Spitzer, & Chevalier (1972); Spitzer (1987); and Kundić & Ostriker (1994) and summarized in Gnedin & Ostriker (1997). Below we review the important results for the disk shocking. The theory of tidal shocking is discussed in detail in Gnedin, Hernquist, & Ostriker (1999). For an alternative linear theory calculation see Weinberg (1994).

In the disk shocking, the phase-averaged first and second order energy changes of stars with the initial energy per unit mass  $E$  are

$$\langle \Delta E \rangle_E = \frac{2 g_m^2 r^2}{3 V^2} A_1(x), \quad (1)$$

$$\langle \Delta E^2 \rangle_E = \frac{4 g_m^2 v^2 r^2 (1 + \chi_{r,v})}{9 V^2} A_2(x), \quad (2)$$

where  $g_m$  is the maximum vertical gravitational acceleration produced by the disk,  $V$  is the vertical component of the cluster velocity with respect to the disk, and  $r$  and  $v$  are the rms position and velocity of stars of energy  $E$ . Here  $\chi_{r,v}$  is the position-velocity correlation factor, which takes values from  $-0.25$  to  $-0.57$  (see Gnedin & Ostriker 1999).

The first order energy change,  $\langle \Delta E \rangle$ , causes reduction in the binding energy of the system and leads to evaporation of the marginally bound stars. The second order change,  $\langle \Delta E^2 \rangle$ , causes a much larger energy dispersion which allows additional stars to leave the cluster. The two effects cooperate and lead to faster dissolution of the cluster.

The adiabatic corrections,  $A_1(x)$  and  $A_2(x)$ , account for conservation of the adiabatic invariants of stars for which the orbital period in the cluster is short compared to the effective duration of the shock,

$$\tau \equiv \frac{H}{V}, \quad (3)$$

where  $H$  is the characteristic scale-height of the disk. The adiabatic corrections can be approximately described as functions of the only dimensionless parameter,

$$x \equiv \omega(r) \tau. \quad (4)$$

Here  $\omega$  is the stellar orbital frequency of stars of energy  $E$  at the rms position  $r$ .

Several approximations have been used to study the adiabatic corrections. (1) The *impulse approximation* is valid for the stars whose motion in the cluster is much slower than the shock,  $x \ll 1$ . This condition applies in the outer regions of the cluster. There both corrections become unity:

$$A_1(x) = A_2(x) = 1, \quad (x \ll 1). \quad (5)$$

(2) The *harmonic approximation* is valid for the stars which oscillate very quickly in a simple harmonic potential and which are not in resonance with the perturbing force. Building on results of Spitzer (1987), we get

$$A_{1S}(x) = e^{-2x^2}, \quad A_{2S}(x) = \frac{9}{4 + 5e^{2x^2}}, \quad (x \gg 1; \text{ no resonances}). \quad (6)$$

Here we have modified the second correction from its version in Gnedin & Ostriker (1997) to make it equal unity for  $x = 0$ . The numeric coefficients are dictated by the asymptotic form for large values of  $x$ . (3)

The *linear theory* by Weinberg (1994) includes the possible resonances and predicts a less steep power-law function. In the limit of large  $\tau$ , the results can be approximated (Gnedin & Ostriker 1999) as:<sup>1</sup>

$$A_{1W}(x) = A_{2W}(x) = (1 + x^2)^{-3/2}. \quad (7)$$

(4) Gnedin & Ostriker (1999) performed *N-body simulations* of the tidal shock, allowing for the self-consistent oscillations of the cluster potential as it relaxes into a new virial equilibrium. The simple fits to the results are

$$A_{1N}(x) = (1 + x^2)^{-5/2}, \quad A_{2N}(x) = (1 + x^2)^{-3} \quad (8)$$

for the “fast shocks” whose durations are comparable to or smaller than the dynamical time at the half-mass radius:  $\tau \lesssim t_{dyn}$ . For the “slow shocks”, the results agree with the predictions of the linear theory (eq. [7]).

In the case of bulge shocking, the Spitzer adiabatic corrections involve a combination of Bessel functions, as described in Gnedin & Ostriker (1997). The Weinberg and *N-body* adiabatic corrections are taken to be the same as for disk shocking. Since the *N-body* simulations of Gnedin & Ostriker (1999) include only disk shocks, further study is needed to determine accurately the adiabatic corrections for bulge shocking.

The first and second order energy changes are of comparable importance. This becomes clear if we define the characteristic shock timescales:

$$t_{sh} \equiv \frac{|E_h|}{dE_h/dt} = P_{\text{disk}} \frac{|E_h|}{\langle \Delta E \rangle_h} \quad (9a)$$

$$t_{sh,2} \equiv \frac{E_h^2}{dE_h^2/dt} = P_{\text{disk}} \frac{E_h^2}{\langle \Delta E^2 \rangle_h}. \quad (9b)$$

Here  $P_{\text{disk}}$  is the period of cluster’s passage through the Galactic disk. The energy changes  $\langle \Delta E \rangle_h$  and  $\langle \Delta E^2 \rangle_h$  are evaluated at the half-mass radius  $R_h$ , and the characteristic energy  $E_h$  is given by the Virial Theorem:  $|E_h| = v_{rms}^2/2 \approx 0.2GM/R_h$  (e.g., Spitzer 1987), where  $M$  is the mass of the cluster. In the impulse approximation we obtain

$$t_{sh} = \frac{3}{4} P_{\text{disk}} \frac{V^2 \omega_h^2}{g_m^2}, \quad t_{sh,2} = \frac{9}{16} P_{\text{disk}} \frac{V^2 \omega_h^2}{g_m^2}, \quad (10)$$

where  $\omega_h \equiv v_{rms}/R_h$  is the rms angular velocity of stars at the half-mass radius. The two timescales are simply related by  $t_{sh,2} = \frac{3}{4} t_{sh}$ , so that both processes contribute similarly to the destruction of the cluster.

### 3. The Fokker-Planck Code

We model the evolution of globular clusters using an orbit-averaged isotropic Fokker-Planck code descended from Cohn (1979, 1980). The code has been modified by Lee & Ostriker (1987) and Lee, Fahlman, & Richer (1991) to include tidal boundary and the three-body binary heating. Stars beyond the tidal boundary do not escape instantaneously but follow instead a continuous distribution function  $f(E)$ , as described in Lee & Ostriker (1987). This accounts for the balance of the internal and external forces at

---

<sup>1</sup>This does *not* imply that the results of Weinberg (1994) for fast shocks are incorrect. The linear theory applies for all values of  $\tau$ , but the final expressions are complex and cannot be fitted simply.

the tidal radius. Therefore, those stars only drift slowly away from the cluster. The tidal field is assumed to be spherically symmetric, which is a weakness of the one-dimensional code (for a discussion see Lee & Goodman 1995). We also assume that the cluster fills its Roche lobe and require that the average density within the tidal radius remain constant throughout the cluster evolution.

The heating of stars which reverses core collapse is provided by three-body binaries. They are included explicitly without following their actual formation and evolution, according to the prescription by Cohn (1985). Ostriker (1985) argued that tidally-captured binaries are probably more dynamically important for massive clusters. Whether tidal capture leads to a hard binary which contributes to stellar ejection after a close encounter or whether it leads (more often) to a merger which causes mass loss following stellar evolution, the outcome is the same. Lee (1987) showed that the merger of stars would give a nearly identical dynamical effect on the cluster because the massive stars formed in the merger would evolve off rapidly. Both processes cause indirect heating by ejecting mass. The situation becomes more complicated if we allow for the existence of primordial binaries and massive degenerate stars. The existence of massive remnant stars, such as neutron stars, could cause three-body binaries to be more important than tidal capture binaries (Kim, Lee & Goodman 1998). However, many aspects of the evolution after core collapse are independent of the actual energy source (Hénon 1961; Goodman 1993).

We include the effects of tidal shocks by modifying the diffusion coefficients in the Fokker-Planck equation. We assume that the first and second order energy changes are known as functions of the energy and position using the results from §2 and Gnedin, Hernquist, & Ostriker (1999). We now re-derive the Fokker-Planck equation in order to define the diffusion coefficients corresponding to the shocks.

Let  $\Psi(E, \Delta E) d\Delta E$  be the probability of scattering of a star of energy  $E$  by the amount  $[\Delta E, \Delta E + d\Delta E]$ .  $N$ -body simulations (Gnedin & Ostriker 1999) show that the probability distribution is nearly Gaussian:

$$\Psi(E, \Delta E) d\Delta E = \frac{1}{\sqrt{2\pi\langle\Delta E^2\rangle}} e^{-\frac{1}{2}\frac{(\Delta E - \langle\Delta E\rangle)^2}{\langle\Delta E^2\rangle}} d\Delta E, \quad (11)$$

where both  $\langle\Delta E\rangle$  and  $\langle\Delta E^2\rangle$  are functions of energy  $E$ . Let  $N(E)dE$  be the number of stars in the energy range  $[E, E + dE]$ . The time evolution of  $N(E)$ , in the absence of two-body relaxation and binary heating, can be described by the following equation

$$N(E, t + \Delta t) = \int N(E - \Delta E, t) \Psi(E - \Delta E, \Delta E) d\Delta E, \quad (12)$$

where the energy changes by the amount  $\Delta E$  in the time interval  $\Delta t$ . Expanding this equation in a series over  $\Delta E$  and  $\Delta t$ , we obtain the usual form of the Fokker-Planck equation

$$\frac{\partial N(E)}{\partial t} = -\frac{\partial}{\partial E} \{N(E) \langle\mathcal{D}_t(\Delta E)\rangle_V\} + \frac{1}{2} \frac{\partial^2}{\partial E^2} \{N(E) \langle\mathcal{D}_t(\Delta E^2)\rangle_V\}, \quad (13)$$

where  $\langle\mathcal{D}_t(\Delta E)\rangle_V$  and  $\langle\mathcal{D}_t(\Delta E^2)\rangle_V$  are the orbit-averaged diffusion coefficients of the first and second order. They are defined by

$$\langle\mathcal{D}_t(\Delta E)\rangle_V \equiv \frac{\int_0^{r_{max}} \langle\mathcal{D}_t(\Delta E)\rangle v r^2 dr}{\int_0^{r_{max}} v r^2 dr}, \quad (14)$$

and

$$\langle\mathcal{D}_t(\Delta E^2)\rangle_V \equiv \frac{\int_0^{r_{max}} \langle\mathcal{D}_t(\Delta E^2)\rangle v r^2 dr}{\int_0^{r_{max}} v r^2 dr}, \quad (15)$$

where  $\langle\mathcal{D}_t(\Delta E)\rangle$  and  $\langle\mathcal{D}_t(\Delta E^2)\rangle$  are the average rates of change of the energy and its dispersion, respectively, per unit volume at a given location  $r$ , and  $r_{max}$  is the maximum radius allowed for a star

of energy  $E$ . Given equations (1) and (2) for the energy changes and equation (11) for their distribution function, we define

$$\langle \mathcal{D}_t(\Delta E) \rangle_{sh} \equiv \int \frac{\Delta E}{\Delta t} \Psi(E, \Delta E) d\Delta E = \frac{\langle \Delta E \rangle}{\Delta t}, \quad (16)$$

$$\langle \mathcal{D}_t(\Delta E^2) \rangle_{sh} \equiv \int \frac{(\Delta E)^2}{\Delta t} \Psi(E, \Delta E) d\Delta E = \frac{\langle \Delta E^2 \rangle + \langle \Delta E \rangle^2}{\Delta t}. \quad (17)$$

The bulge and disk tidal shocks are applied at the time step when the cluster is at its perigalacticon or crosses the Galactic disk, respectively. The diffusion coefficients are normalized to the current time step,  $\Delta t$ , so as to produce the right amount of heating per event. The shocks are repeated every orbital period of the cluster.

The time step was chosen such that both the cluster mass and the central density change by no more than 1% between time steps:

$$\Delta t = 0.01 \times \min[(d \ln \rho / dt)^{-1}, (d \ln M / dt)^{-1}]. \quad (18)$$

Lee & Ostriker (1993) suggested that such a time step should be sufficient for an accurate calculation of the cluster evolution, both before and after core collapse. We compare our results without tidal shocking with those of Quinlan (1996), who used the same time step for the potential re-computation but broke it down into 32 sub-steps for updating the distribution function (the ‘‘Fokker-Planck steps’’). We found a measurable difference in the core collapse times only for very concentrated clusters, with the initial concentration  $c \gtrsim 2.5$ . For these clusters an even smaller time step may be required, although our results never differ by more than 30% (cf. Figure 17).

As described below, in order to incorporate correctly the effects of tidal shocks into the code, the shock diffusion coefficients should be applied separately from the relaxation terms, and the potential should be recomputed accordingly thereafter (an alternative approach has been suggested by Johnston, Hernquist & Weinberg 1998). It seems awkward, though still possible, to include a set of Fokker-Planck steps for every potential time step in this scheme, as Quinlan (1996) did for the isolated clusters. We chose not to do so and therefore we had the potential updated every time the distribution function was changed. Since our time step (eq. [18]) gives very good accuracy for most of the computed cluster models, we did not change it specifically for high concentration clusters. The resulting error should in any case be small.

The alternative implementation of tidal shocks in a Fokker-Planck code has been done by Murali & Weinberg (1997a-c). Those authors employ the linear theory formalism of Weinberg (1994) and calculate the change of the distribution function directly from the Boltzmann equation. That approach is more accurate but is more cumbersome. Since the linear theory expressions are supported by the restricted  $N$ -body simulations (Weinberg 1994), that method and our derived adiabatic corrections should give the same result. The work of Murali & Weinberg has focused more on the destruction time of globular clusters under various assumptions and on predicting the initial cluster distribution. In this paper, in addition to obtaining fitting formulae for the destruction time we present also the detailed evolution of individual clusters and compare it with previous work on isolated clusters.

### 3.1. Comparison with $N$ -body simulations

Gnedin & Ostriker (1999) report self-consistent  $N$ -body simulations of a single disk shock of various strengths and durations. The cluster is modeled as a low-concentration King-model ( $c = 0.84$ ) with a

realistic number of particles,  $N = 10^6$ . The characteristic disk shocking strength is low and most of the stars remain bound to the cluster. However, the energy distribution changes in response to the perturbation. The resulting distribution after the virialization phase is accurately fitted by equations (1), (2), and (8). Although the result depends on the initial structure of the cluster, the above fits still apply for the more concentrated cluster with  $c = 1.5$  (see Gnedin & Ostriker 1999 for more details).

The  $N$ -body modeling of tidal shocks is intrinsically more accurate than the Fokker-Planck formulation. The former takes into account the non-linear virialization following the shock and the anisotropic effects induced by disk shocking. A direct comparison of the resulting energy changes between the two codes is difficult because of the algorithmic differences. Therefore, we have taken the simple approach to reproduce the  $N$ -body results in our F-P code as closely as possible.

The general procedure for advancing the distribution function (DF) in time consists of two parts (Cohn 1979). The first part introduces the first and second order changes of the DF as a solution of the Fokker-Planck equation. The second part updates the cluster potential by solving Poisson’s equation with the density following from the new DF. During the second step, the DF is kept constant as a function of the stars’ adiabatic invariants and therefore it changes as a function of energy. This procedure is no longer correct when treating tidal shocks which last of the order of the dynamical time of the cluster. This timescale is short enough that adiabatic invariants may themselves change.

We find that in order to reproduce the  $N$ -body results, we need to modify the above procedure for tidal shocks. During the time step when the cluster passes through the Galactic disk or close to the Galactic center, we first apply the shock diffusion coefficients and update the DF. Then we fix the DF as the function of energy and obtain the new potential by solving Poisson’s equation. Specifically, since the potential is changed and the energy grid is renormalized, we require that in each energy bin the new energy distribution,  $N_{new}$ , scale with the new energy grid,  $E_{new} = E + \Delta E$ , as

$$N_{new}(E_{new}) dE_{new} = N(E) dE, \quad (19)$$

where  $N(E)$  is the energy distribution before the potential recalculation. We have checked that the above procedure reproduces well the  $N$ -body results for a range of shock amplitudes. Figure 1 shows the change in the energy distribution after a single shock in a test cluster. The agreement between the Fokker-Planck and  $N$ -body results is reasonably good. Also, Figure 1 shows that the previous procedure for updating the DF for the fixed adiabatic invariants departs much more strongly from the  $N$ -body results than does our new prescription.

Another effect demonstrated by the  $N$ -body simulations is a slight decrease in the shock-induced energy dispersion subsequent to and caused by the potential fluctuations following the shock. This paradoxical “refrigeration effect” persistently survived all our tests and seems to be real (see Gnedin & Ostriker 1999). However, the magnitude of the dispersion decrease is relatively small, which led us to ignore it in the present calculation. Once the nature of this effect is understood better, it should also be included in the models of globular clusters.

#### 4. Typical Evolution of a Single Cluster

We consider now the detailed models of the globular cluster evolution. For the most part, we study single-mass models and then briefly investigate the effect of a spectrum of stellar masses.

With the new data on proper motions from *Hipparcos*, it is now possible to reconstruct full three-

dimensional velocities for some of the Galactic globular clusters (Odenkirchen et al. 1997) and to build realistic models of their evolution. We use the inferred orbital parameters for NGC 6254 and calculate its orbits in an analytic potential of the Galaxy from Allen & Santillan (1991). The orbits are of the rosette type (Figure 2) with a small eccentricity,  $e = 0.21$ . The cluster moves around the Galaxy with a period of about  $1.4 \times 10^8$  yr, during which it passes next to the Galactic center every  $9.5 \times 10^7$  yr and crosses the Galactic disk every  $5.3 \times 10^7$  yr. The period ratio differs from the expected factor of two due to the slow precession of the orbit.

From the computed orbits of NGC 6254 we infer that the amplitude of tidal shocks varies approximately as a Gaussian function of time. This satisfies the conditions under which the  $N$ -body adiabatic corrections were calculated (see Gnedin & Ostriker 1999).

#### 4.1. Single Mass Models

The observed structure of NGC 6254 is well characterized by a King model (King 1966) with the concentration  $c = 1.4$ , or the structural parameter  $W_0 = 6.55$ . The mass of the cluster is  $2.25 \times 10^5 M_\odot$ , assuming a constant mass-to-light ratio  $M/L_V = 3$  in solar units. First, we consider in detail a model composed of stars of the same mass,  $m_* = 0.7 M_\odot$ . The important parameters of the model are summarized in Table 1.

We implement both disk and bulge shocks in our integration. The models differ in the way the shocks are included: no tidal shocks, steady tidal field and relaxation only (*case 0*); tidal shocks with the first order  $\langle \Delta E \rangle$  term only (*case 1*); tidal shocks with the second order  $\langle \Delta E^2 \rangle$  term only (*case 2*); and finally tidal shocks with both  $\langle \Delta E \rangle$  and  $\langle \Delta E^2 \rangle$  terms (*case 3*).

An important observable of the cluster evolution is the mass-loss due to tidal shocks and due to the direct escape of high-velocity stars. Figure 3 shows the run of the cluster mass with time. As is well-known, the mass of a tidally limited cluster goes to zero in an approximately linear fashion. A convenient choice is to express time  $t$  in the units of the initial half-mass relaxation time  $t_{rh,0}$  (eq. [21]). Two-body relaxation leads to destruction of the cluster in about  $32 t_{rh,0}$ . Note that the numerical problems cause the cluster to lose its stability and dissolve into the sea of background stars before its mass reaches exactly zero. Usually the code fails to re-calculate the cluster potential when the mass falls to about 1% – 4% of the initial mass. However, we can extrapolate through the last few time steps in order to estimate the hypothetical time when the cluster mass vanishes. The disruption time obtained this way is an overestimate of the real disruption time, but all other estimates would suffer from a personal choice. Thus, in the rest of the paper we use the extrapolation of our calculations as the destruction time  $t_d$ .

The destruction time is significantly reduced when we include gravitational shocks. The  $\langle \Delta E \rangle$  term alone changes  $t_d$  from  $32 t_{rh,0}$  to  $26 t_{rh,0}$  and the shock-induced relaxation brings it to about  $24 t_{rh,0}$ . To access the importance of the two shock terms separately, we turn off the energy shift,  $\langle \Delta E \rangle$ , for the *case 2* run. The second order term leads to an enhanced mass loss relative to the relaxation case for most of the evolution. This effect is not as strong as the first order effect due to the limiting adiabatic corrections, which we investigate in more detail later<sup>2</sup>. For comparison, we also show the mass loss that would have been due to the shock-induced relaxation if there were no adiabatic corrections (the impulse approximation). The latter effect would reduce the destruction time of the cluster by about a half.

---

<sup>2</sup>The effect of the second order term is reduced relative to the results of Gnedin & Ostriker (1997) by inclusion of the



An important feature of tidal shocks is the enhanced mass loss at the early stages of the evolution, prior to core collapse. In the pure relaxation case, the mass loss is slow until core collapse and linear in time afterwards. The first theoretical calculations of the probability of stars’ escape from the cluster through two-body relaxation (Ambartsumian 1938; Spitzer 1940) predicted the following dimensionless rate

$$\xi_e \equiv -\frac{t_{rh}(t)}{M(t)} \frac{dM}{dt} = 0.0074, \quad (20)$$

where  $t_{rh}$  is the half-mass relaxation time (Spitzer & Hart 1971):

$$t_{rh} = 0.138 \frac{M^{1/2} R_h^{3/2}}{G^{1/2} m_* \ln(\Lambda)}. \quad (21)$$

Here  $M$  is the current cluster mass,  $R_h$  is the half-mass radius,  $m_*$  is the average stellar mass, and  $\ln(\Lambda) = \ln(0.4N)$  is the Coulomb logarithm,  $N$  being the number of stars in the cluster. Later calculations of the tidally-truncated cluster by Hénon (1961) gave a larger value,  $\xi_e \approx 0.045$ .

Spitzer & Chevalier (1973) used Monte-Carlo simulations for several models of globular clusters and found  $\xi_e = 0.05$  for  $R_t/R_h = 3.1$ , and  $\xi_e = 0.015$  for  $R_t/R_h = 9.3$ , where  $R_t$  is the tidal radius of the cluster. Based upon those simulations, Aguilar, Hut, & Ostriker (1988; hereafter AHO) proposed the following fitting formula for the time to disruption:

$$t_d = \left(0.15 \frac{R_h}{R_t}\right)^{-1} t_{rh,0}, \quad (22)$$

where  $t_{rh,0}$  is the initial relaxation time. For NGC 6254, the disruption time predicted by AHO would be about  $52 t_{rh,0}$ , whereas we see that the cluster dissolves in  $32 t_{rh,0}$  even without tidal shocks. In general, we find that equation (22) overestimates the actual disruption time by a factor of several.

We compare the previous results for the escape probability  $\xi_e$  with our Fokker-Planck calculations in Figure 4. In the relaxation model (*case 0*), the value of  $\xi_e$  rises almost monotonically through core collapse and until destruction of the cluster, reaching and exceeding Hénon’s estimate only in the late stages of the evolution. On the contrary, in the shock-dominated models the escape probability is very high in the beginning when tidal shocks efficiently remove stars from the outer parts of the cluster. The mass loss then slows down and conforms to the relaxation rate soon before core collapse. Then again,  $\xi_e$  rises with time to reach Hénon’s self-similar value. This later increase caused primarily by the declining mass of the cluster, since the mass loss rate is almost constant in the post core-collapse cluster.

The cluster structure can be described in terms of the characteristic radii, such as the *core radius*, reflecting compactness of the cluster; the *tidal radius*, confining all stars bound to the cluster; and the *half-mass radius*, relating to the global properties of the cluster. Figure 5 shows the evolution of these parameters normalized to the initial core radius. The core radii for all models drop to extremely small values at the point of core collapse. The core-collapse time  $t_{cc}$  is about  $13 t_{rh,0}$  for the relaxation case, in agreement with Lee & Ostriker (1987) and Quinlan (1996). Tidal shocks speed up core collapse significantly:  $t_{cc} = 10 t_{rh,0}$  in *case 1* and it is still smaller when we include the shock-induced relaxation term. The half-mass radius changes only by a factor of two over the whole cluster lifetime, which indicates that core

---

correlation factor  $(1 + \chi_{r,v})$  (eq. [2]). At each time step, we calculate the value of  $\chi_{r,v}(E; c)$  using the fitting formula from Gnedin & Ostriker (1999).

collapse affects only a small fraction of stars. The tidal radius decreases slowly, reflecting the gradual mass loss from the cluster.

Figure 6 illustrates core collapse more clearly. The central density of the cluster,  $\rho_c$ , rises by nine orders of magnitude before the collapse is halted by a production of three-body binaries in the very dense core of the cluster. The energy released from the binaries eventually reverses the collapse. The cluster consequently expands, though the central density still remains very high (about four orders of magnitude higher than initially). The actual value of  $\rho_c$  at the core bounce and post-collapse phase depends on the specific heating mechanism. A stronger heating rate gives a lower central density during the post-collapse phase.

The cluster concentration,  $c \equiv \log_{10}(R_t/R_c)$ , is closely related to the central density. Since the tidal radius  $R_t$  decreases slowly with time as  $M^{1/3}$ , the concentration varies roughly as  $\log \rho_c$ .

The core collapse time provides a very useful yardstick for cluster evolution. Even in the presence of tidal shocks, the evolution of the models is similar when the units of time are scaled to the core collapse time. Figure 7 illustrates this point. The central density in models *0–3* varies almost identically with  $t/t_{cc}$ . Therefore, we can use this scaling to parameterize cluster evolution. The destruction time is an almost constant multiple of the core collapse time:  $t_d \approx 2.5 t_{cc}$ .

The post-collapse evolution of globular clusters depends on the concentration and the remaining mass. The self-similar solution by Hénon (1961) for tidally-limited clusters can be expressed (Goodman 1993) as follows:

$$t_d - t = 22.4 t_{rh}(t), \quad (23)$$

where  $t_d - t$  is the time to disruption at time  $t$ . Figure 8 shows that the self-similar limit is approached at late stages of the cluster evolution, but for the most part equation (23) underestimates the time to destruction by about 50%.

#### 4.1.1. Comparison of adiabatic corrections

An important constituent of our models is adiabatic corrections for the tidal shock effects (eqs. 6–8). Various corrections predict different impact of shocks in the middle parts of clusters and lead to different evolutionary paths. The amplitude of the corrections depend on the ratio of the perturbation timescale to the dynamical time of stars in the cluster. For NGC 6254, the characteristic time for disk shocking (eq. [3]) is  $\tau_{\text{disk}} = 1.3 \times 10^6$  yr, and for bulge shocking (cf. Gnedin, Hernquist, & Ostriker 1999) is  $\tau_{\text{bulge}} = 1.3 \times 10^7$  yr. The half-mass dynamical time of the cluster is initially much shorter,  $\omega_h^{-1} = 3.1 \times 10^5$  yr, leading to strong suppression of the effects of tidal shocks.

Figure 9 compares the Spitzer, Weinberg, and  $N$ -body adiabatic corrections for the *case 3* models of NGC 6254. When the shocks are “slow” ( $x = \omega_h \tau \gg 1$ ), as indicated by the true values of  $\tau_{\text{disk}}$  and  $\tau_{\text{bulge}}$ , both *S1* and *N1* models have tidal shock effects suppressed more strongly than does the *W1* model with the less steep adiabatic corrections. For the “slow” shocks, the *W1* model gives the correct description of the cluster evolution.

When we decrease the shock timescales by a factor of five, we enter the regime of “fast shocks” and the *N2* model is correct. For  $x \lesssim 1$ , we can estimate the importance of the adiabatic corrections by the Taylor expansion of equations (6–8). The *N2* model shows the slowest evolution because  $A_{1N} \approx 1 - 2.5x^2$ , whereas for the *W2* model,  $A_{1W} \approx 1 - 1.5x^2$ . Even though the first order correction for the *S2* model,

$A_{1S} \approx 1 - 2x^2$ , is smaller than  $A_{1W}$ , the second order correction is larger,  $A_{2S} \approx 1 - 1.1x^2$ . This allows the  $S2$  model to evolve faster than the other two.

Finally, when we reduce the shock timescales by a factor of hundred, the impulse approximation applies everywhere in the cluster and all three models are essentially identical. The evolution in this case proceeds much faster: the cluster is destroyed in half the time of the original model  $W1$ . Thus, adiabatic corrections are critical for calculating correct globular cluster models.

#### 4.1.2. Low concentration model

For comparison, we consider another model of NGC 6254, with lower concentration  $c = 0.84$ , or  $W_0 = 4$ . This is the model used for  $N$ -body simulations of Gnedin & Ostriker (1999). All other parameters are the same as in the previous model. We keep the observed tidal radius in parsecs, so the core radius and the relaxation time scale in physical units accordingly (see Table 1). Therefore, both models have the same average density,  $\rho_{av} \propto M/R_t^3$ .

Figure 10 shows the mass evolution of the low concentration model. The cluster evaporates much faster than the high concentration model, in units of the initial relaxation time  $t_{rh,0}$ . Clearly, tidal shocks have much stronger effect on less concentrated clusters but the total speed-up in time to destruction, due to shocks, is again about 25%. Notice that the destruction time in years is about the same for the low- and high-concentration models. Figure 11 shows that the evolution of the central density is qualitatively similar to the previous model. However, the effect of the tidal shock relaxation is stronger for the low-concentration model.

## 4.2. Multi-mass models

In a single mass model, the energy is transferred between the cluster core and the envelope, which requires a conduction mechanism acting on the half-mass relaxation timescale. In a multi-mass model, the energy exchange occurs also between stars of different mass. A typical timescale for the energy exchange between the two mass species  $m_1$  and  $m_2$  (where  $m_2 < m_1$ ) is  $t_{rh} \times (m_2/m_1)$ . Since this is much shorter than the core collapse time for single mass clusters, the overall evolution of multi-mass clusters is expected to be faster.

Lee & Goodman (1995), for example, considered the evaporation of a multi-mass cluster in a steady tidal field and found that the mass loss rate can more than double relative to the single-component case. Chernoff & Weinberg (1990) investigated the effects of stellar evolution on the cluster dynamics. In the future, it will be important to generalize the present calculations by including a realistic mass function and stellar evolution, along with the presently implemented two-body relaxation and tidal shocks. In this paper, we present only an illustrative model allowing for the mass spectrum.

We take the previously described model for NGC 6254 and include seven mass components, ranging from  $0.1M_\odot$  to  $0.7M_\odot$ . The number of stars in each component  $N(m) \propto m^{-2}$ . Thus, the upper mass limit corresponds to the turn-off of the main sequence at 10 billion years (we also used it in the single-mass models), and the lower limit is a reasonable cutoff of the initial mass function. The relaxation time is defined by equation (21), where we substitute for  $m_*$  the mean stellar mass (see Lee & Goodman 1995).

Figure 12 shows the mass loss for the multi-mass model. Notice that although the evolution proceeds faster in units of the initial half-mass relaxation time, this timescale expressed in years is longer than that for the single-component model (Table 1). As a result, the destruction time is roughly 20 Gyr in both cases. The contribution of tidal shocks in the multi-mass model is greater, reducing the time to destruction by about 37%.

#### 4.2.1. Comparison with $N$ -body models

Recent paper by Takahashi & Portegies Zwart (1998) compares the multi-mass two-dimensional Fokker-Planck (F-P) models of Takahashi (1995) with the  $N$ -body simulations using a special purpose computer, *GRAPE-4*. The models include stellar evolution, two-body relaxation, and the tidal truncation for a low concentration ( $c = 0.67$ ) cluster model from Chernoff & Weinberg (1990). The above authors argue that the escape of stars through the tidal boundary in an isotropic F-P code, where the distribution function depends only on the energy, is faster than in the  $N$ -body models. To remedy this disagreement, they suggest a new escape criterion based both on the energy and angular momentum of stars. This “apocenter” criterion can only be implemented in the anisotropic F-P code of Takahashi, Lee, & Inagaki (1997).

The old isotropic and the new anisotropic escape criteria lead to significantly different results only when the mass loss rate per relaxation time is high. This especially affects the early stages of the cluster evolution, when stellar winds from young massive stars drive mass loss on a relatively short timescale. Immediate removal of that mass in the Chernoff & Weinberg (1990) models lead to the disagreement with the  $N$ -body simulations (see Takahashi & Portegies Zwart 1998). Since our models do not include stellar evolution, we expect less disagreement.

We run a *case 0* model of the cluster using the parameters from Chernoff & Weinberg (1990). We use 14 mass components from  $0.4M_{\odot}$  to  $15M_{\odot}$ , distributed according to the specified mass function,  $N(m) \propto m^{-2.5}$ . Without stellar evolution the time to destruction in our model should be longer than in the  $N$ -body and the anisotropic F-P models which give  $t_d \approx 1.3t_{rh,0}$ . Indeed, we find that our model evolves slower, with  $t_d \approx 2t_{rh,0}$ . This indicates that our results represent an upper limit on the destruction times of globular clusters.

## 5. Review of Globular Cluster Evolution Including Tidal Shocks

The evolution of the isolated single-mass King models (in dimensionless units) is determined by the only parameter, the concentration  $c$ . Inclusion of tidal shocks introduces another independent parameter, for example, the ratio of the half-mass relaxation time to the characteristic shocking time,

$$\beta \equiv t_{rh}/t_{sh}. \quad (24)$$

The parameter  $\beta$  is a combination of two variables describing the structure of clusters: the number of stars,  $N$ , and the characteristic density,  $\rho_h \propto M/R_h^3$ . When the amplitude of the tidal force on the cluster is fixed, the shocking time (eq. [10]) scales as  $t_{sh} \propto \rho_h$ , and the relaxation time (eq. [21]) scales as  $t_{rh} \propto \rho_h^{-1/2} N/\ln \Lambda$ , where  $\Lambda = 0.4N$ . Then

$$\beta \propto \frac{N}{\ln \Lambda} \rho_h^{-3/2}. \quad (25)$$

While the concentration  $c$  describes the effects of two-body relaxation, the parameter  $\beta$  shows the relative importance of tidal shocks. In this Section, we explore the evolution of globular clusters for a wide range of initial parameters  $c$  and  $\beta$ .

All models in this section include fully the relaxation and tidal shock effects (i.e., *case 3*) with the adiabatic corrections for “slow shocks”, equation (7). We arrange a grid of initial conditions, covering a number of cluster concentrations, from  $c = 0.6$  to  $c = 2.6$  with the step 0.2, and a range of shock parameters,  $\beta$ . We compute 15 models per concentration family, equally spaced on the logarithmic scale from  $\beta \approx 10^{-5}$  to  $\beta \approx 10^2$ . All other parameters correspond to the model of NGC 6254 described in the previous section. The observed tidal radius of NGC 6254 is fixed and the core radius scales accordingly with the concentration. Thus all models have initially the same average density,  $M/R_t^3$ .

### 5.1. Cluster evolution in figures

Figure 13 shows how different regimes of cluster evolution map on the plane of parameters  $c$  and  $\beta$ . In the lower left region of the plot tidal shocks are weak and evolution is dominated by two-body relaxation; in the upper left region core collapse proceeds on a relatively short timescale without affecting most of the cluster; and in the lower right region tidal shocks are strong and cause substantial mass loss before core collapse. The upper right region is never reached in reality because of extremely strong tidal shocks leading to fast destruction of the clusters.

Qualitative evolution in the left region of the plane is characteristic of a tidally-truncated model. As clusters start to collapse, the relaxation time becomes increasingly shorter and the tidal shock time becomes increasingly longer because the mean density  $\rho_h$  rises (Figure 14). The mass loss is weak at this stage and the number of stars,  $N$ , stays relatively constant. As a result, the parameter  $\beta$  decreases (and moves to the left of the diagram) until the very advanced stages of core collapse. At that point the value of  $\beta$  freezes and the evolutionary tracks are strictly vertical (the upper part of the diagram). After core collapse, the cluster re-expands and its density falls slightly, moving it to the right of the  $c - \beta$  diagram. At a later time, so little mass is left that two-body relaxation speeds up again and drives clusters to complete dissolution.

Figure 15 illustrates the behavior of the parameter  $\beta$  with time. On the low end, all lines scale similarly, following the evolution of the mean density. For the large initial values of  $\beta$ , the early mass loss due to shocks is very important. This leads us to investigate the right part of the  $c - \beta$  diagram.

The evolution of clusters with strong tidal shocks differs dramatically from the previous case. An early mass loss caused by the shocks changes the structure of the clusters, removing stars from the outer parts and adding energy dispersion in the core. This increases the central and the mean density of the clusters. Both core collapse and final destruction proceed much faster. These effects of tidal shocks leave noticeable ripples in the clusters tracks on the right part of the diagram (Figure 13).

Tidal shocking is rapidly self-limiting. Clusters with large values of  $\beta$  quickly lose mass and evolve to  $\beta \lesssim 0.1$ . Figure 15 demonstrates that just a first few shocks lower the value of  $\beta$  by several orders of magnitude. Every subsequent shock causes the see-saw variations of the shock parameter, with an increasing amplitude towards the late stage of evolution when fewer stars are left.

A few clusters in the right part of the  $c - \beta$  diagram cross their evolutionary tracks on the way to core collapse. At the time of crossing, at least one of the clusters has already suffered a severe mass loss caused by the shocks and has a structure significantly deviating from King models. The density profiles of the two

clusters are similar within the half-mass radii but depart from each other closer to the tidal radius. Those clusters with higher initial concentration and stronger shocks are more severely truncated than the clusters with smaller concentration and weaker shocks. Also, tidal shocks add the velocity dispersion in the core and, therefore, raise the central density so that the ratio  $R_t/R_c$ , as measured by the concentration  $c$ , is the same for both clusters.

At the crossing point the two parameters,  $c$  and  $\beta$ , no longer uniquely specify cluster’s future path. A third parameter comes into play as we investigate the thermodynamics of clusters.

## 5.2. Cluster thermodynamics

From a thermodynamic point of view, we can consider stars as particles of gas. A critical factor determining evolution is the heat flow between the core and the halo of the cluster. The heat in this case is the velocity dispersion of stars,  $T \equiv v_m^2$ , whose flux is derived in Spitzer (1987, p. 68). The amount of heat transported through the cluster per unit time, or the “luminosity”, is  $4\pi r^2 F(r)$ . The heat conduction facilitates core collapse and proceeds on a relaxation timescale. Let us construct a new dimensionless ratio of the heat transported through the half-mass radius in the relaxation time  $t_{rh}$ , to the total reservoir of heat,  $T(r_h)$ . Neglecting constant factors of order unity, we define the following parameter

$$\gamma \equiv - \left. \frac{d \ln v^2}{d \ln r} \right|_{r_h}, \quad (26)$$

which is essentially a logarithmic gradient of the velocity dispersion. For an isothermal sphere,  $\gamma = 0$ . In general, for clusters on the way to core collapse, this parameter is positive as the heat is transferred from the kinematically hot core to the cold halo and grows as core collapse accelerates. In contrast, tidal shocks try to reverse the heat flow by heating preferentially the outer parts of the cluster. Even though the instantaneous value of  $\gamma$  is determined only by the density structure, its derivative,  $\dot{\gamma}$ , is a signature of the relaxation– or the tidal shock–driven evolution.

The clusters crossing paths on the  $c - \beta$  diagram have similar values of  $\gamma$ , but the derivatives have opposite sign. For the clusters moving almost vertically on the diagram  $\dot{\gamma} > 0$ , whereas for the clusters which cross the diagram horizontally  $\dot{\gamma} < 0$ . Therefore, the evolution of the former is dominated by two-body relaxation and of the latter by tidal shocks.

Knowing the value of  $\dot{\gamma}$  for the Galactic globular clusters, we could in principle differentiate the two evolutionary paths. Unfortunately, it is hard to establish the sign of  $\dot{\gamma}$  observationally.

Another signature of the tidal shock–dominated clusters is a steep density profile and a low number density of stars at the tidal radius. Strong shocks sweep away a large number of stars at once and leave the cluster filling smaller volume in space than the Roche lobe imposed by the external tidal field. Clusters with a sharp density contrast and a high velocity dispersion of the halo stars might be experiencing strong shocking. Most of such clusters are expected to come close to the Galactic center but are not necessarily present there now.

### 5.3. Cluster evolution in numbers

The mass loss from clusters is strongly enhanced by tidal shocks. An illustration of this is the fraction of the initial mass remaining at the time of core collapse,  $M(t_{cc})$ . Figure 16 shows that the larger  $\beta$ , the smaller the remaining mass. Note, that many models of various initial concentration converge at  $\beta \approx 0.1$ , giving  $M(t_{cc}) \approx 45\%$ .

The core collapse time is a strong function of both initial parameters  $c$  and  $\beta$ . Figure 17 shows  $t_{cc}$  for the models without tidal shocks. In units of the initial half-mass relaxation time, the core collapse time can be fitted as follows:

$$\frac{t_{cc}}{t_{rh,0}} = f_1(c) \equiv 10^{a_1 + a_2 c + a_3 c^2 + a_4 c^3 + a_5 c^4}, \quad (27)$$

where the coefficients  $a_i$  are given in Table 2. Our results are in good agreement with Quinlan (1996), except for the clusters with very high concentration. Even for them, the maximum difference in  $t_{cc}$  is less than 30%.

Figure 18 shows the core collapse time for the models including tidal shocks. The shock-induced relaxation speeds up core collapse by adding velocity dispersion in the core and by removing stars in the outer parts of the clusters, thus reducing the relaxation time. We fit the results assuming, as an *Ansatz*, the following functional form:

$$\frac{t_{rh,0}}{t_{cc}} = \left. \frac{t_{rh,0}}{t_{cc}} \right|_{\beta=0} (1 + b_1 \beta^{b_2} + b_3 \beta^{b_4}). \quad (28)$$

The coefficients  $b_i$  for models of various concentration  $c$  are given in Table 3. The fit is generally accurate to 20%, with larger errors for models with very high initial concentration.

The time to destruction,  $t_d$ , is also strongly affected by tidal shocks. As we have emphasized in the previous section, evolution of clusters with different parameters scales similarly when time is normalized to the core collapse time. Accordingly, we provide the fitting formulae for the scaled destruction time,  $t_d/t_{cc}$ . For the models without tidal shocks (Figure 19), we use the same functional form as equation (27) and fit  $t_d$  both in units of the initial relaxation time and in units of the core collapse time:

$$\frac{t_d}{t_{rh,0}} = f_2(c), \quad \frac{t_d}{t_{cc}} = f_3(c), \quad (29)$$

where the coefficients  $a_i$  are again given in Table 2.

For the models including tidal shocks (Figure 20), the scaled destruction time varies very little for the low concentration clusters and increasingly more for the high concentration ones. Interestingly enough, regardless of the initial structure, models with strong shocks converge to an almost constant value  $t_d/t_{cc} \sim 2$ . It follows that the core collapse time is a midpoint in cluster's lifetime.

Since the value of  $t_d/t_{cc}$  is almost constant for  $\beta \ll 1$  and for  $\beta \gg 1$ , we choose the following functional form to fit the results:

$$\frac{t_d}{t_{cc}} = \left. \frac{t_d}{t_{cc}} \right|_{\beta=0} \left( \frac{1 + d_1 \beta^{d_2}}{1 + d_3 \beta} \right), \quad (30)$$

where the coefficients  $a_i$  are given in Table 4. This expression allows for a variation in the slope of the fit for large values of  $\beta$ , but the coefficient  $d_2$  is always close to unity, as expected.

In the case of very strong shocks, both the core collapse and the destruction times scale approximately as  $t_{cc}, t_d \propto \beta^{-1/2}$  (cf. the coefficient  $b_2$  in Table 3). This asymptotic behavior can be understood as follows.

The shock parameter  $\beta$  is proportional to the mean energy change due to shocks (eq. [9]), which in turn is proportional to the amplitude of the tidal force squared,  $I^2$ . Therefore, the approximate scaling of  $t_{cc}$  and  $t_d$  indicate that these timescales vary inversely proportional to  $I$ .

## 6. Discussion

Our Fokker-Planck models provide the most comprehensive calculations of the globular cluster evolution including gravitational tidal shocks. We find that tidal shocks significantly alter the evolution, in agreement with the earlier studies by Spitzer & Chevalier (1973) and more recent ones by Gnedin & Ostriker (1997) and Murali & Weinberg (1997a-c). Globular clusters appear to be rather fragile with regard to the effects of tidal shocking.

Tidal shocks accelerate dynamical evolution and evaporation of clusters by effectively stripping stars in the outer regions and adding energy dispersion in the core. These effects are self-limiting: as clusters lose mass and become more compact, the relative importance of tidal shocks rapidly diminishes in favor of two-body relaxation. In the case of the Galactic globular cluster NGC 6254, tidal shocks decrease the destruction time from 24 Gyr to 18 Gyr.

We examine several types of adiabatic corrections: the harmonic approximation (of L. Spitzer), the linear perturbation theory (of M. Weinberg), and the results of the  $N$ -body simulations. The differences between the various types of adiabatic corrections depend on the regime of “slow shocks” or “fast shocks”, but overall the corrections are critical for accurate calculation of the evolution. Without adiabatic corrections, the destruction time of NGC 6254 is twice as short.

The evolution of models with a single mass component can be characterized by the King-model concentration parameter,  $c$ , and the shock parameter,  $\beta$  (eq. [24]). The effects of tidal shocks are important when  $\beta \gtrsim 10^{-3} - 10^{-2}$ , depending on the concentration. Tidal shocks increase both the mean and the central densities, relative to the relaxation case. Core collapse is accelerated by about 30% for  $\beta = 0.01$  and by a factor of 3 for  $\beta = 1$ . In the limit of strong shocks, the core collapse time scales approximately as  $t_{cc} \propto \beta^{-1/2}$ . The time to destruction is also dramatically reduced, following the same scaling law. Overall, we find that evolution of models proceeds very similarly when time is expressed in units of the core collapse time. In the limit of strong shocks, the destruction time  $t_d \approx 2 t_{cc}$ , independently on the initial concentration. Core collapse provides a useful midpoint of cluster evolution.

We also consider an illustrative model with a range of stellar masses. In units of the initial relaxation time, the evolution proceeds much faster than in the single-mass case, but for both models the time to destruction is comparable when expressed in years. Thus, the models with the same average density evolve in approximately the same time. A systematic study of multi-mass models is beyond the scope of the present study and requires a knowledge of the initial mass function in star clusters.

The results of our calculations have important implications for the evolution of globular clusters. For the sample of the Galactic globular clusters from Gnedin & Ostriker (1997) the typical values of the shock parameter are  $\beta \sim 10^{-3} - 10^{-2}$ . This indicates that the effects of tidal shocks and of two-body relaxation are comparable at present. Since the shock effects quickly saturate, tidal shocks must have been more important in the past. Not only will the current population of clusters be significantly depleted in the future (Gnedin & Ostriker 1997), but also a large fraction of the initial population might have been already destroyed in the Galaxy (Murali & Weinberg 1997c).



Present calculations can be improved in several ways. A reasonable mass function and effects of stellar evolution should be included in order to accurately describe the early phase of cluster evolution. Also, in our treatment of tidal shocks we have neglected small (but real) negative relaxation due to cluster oscillations. The final weakness of our models is the assumption of the isotropic velocity distribution. Radial anisotropy would develop in the outer parts in the absence of tidal shocks. Since the stars on radial orbits will be ejected more easily than those on circular orbits, tidal shocks should effectively isotropize orbits even in the outer parts. Takahashi (1995,1997) and Takahashi, Lee, & Inagaki (1997) have developed an accurate method for integrating the anisotropic Fokker-Planck equation. We plan to include the effect of tidal shocks in the anisotropic code in order to clarify these points.

We would like to thank Kathryn Johnston for useful discussions, and the anonymous referee and the scientific editor Steven Shore for detailed comments. This work was supported in part by NSF grant AST 94-24416 and by Korea Science and Engineering Foundation grant No. 95-0702-01-01-3.

## REFERENCES

- Aguilar, L., Hut, P., & Ostriker, J. P. 1988, *ApJ*, 335, 720
- Allen, C., & Santillan, A. 1991, *RMxAA*, 22, 255
- Ambartsumian, V. A. 1938, *Uch. Zap. L.G.U.*, 22, 19. English transl. in *IAU Symposium 113, Dynamics of Star Clusters*, ed. J. Goodman, & P. Hut (Dordrecht: Reidel), 521
- Antonov, V. A., 1962, *Vestnik Leningrad University*, 7, 135. English transl. in *IAU Symp. No. 113, Dynamics of Star Clusters*, ed. J. Goodman, & P. Hut (Dordrecht: Reidel), 525
- Ashman, K. M., & Zepf, S. E. 1998, *Globular Cluster Systems* (Cambridge: Cambridge University Press)
- Chernoff, D. F., & Shapiro, S. L. 1987, *ApJ*, 322, 113
- Chernoff, D. F., & Weinberg, M. D. 1990, *ApJ*, 351, 121
- Cohn, H. N. 1979, *ApJ*, 234, 1036
- Cohn, H. N. 1980, *ApJ*, 242, 765
- Cohn, H. N. 1985, in *Dynamics of Star Clusters*, *IAU Symposium 113*, ed. J. Goodman, & P. Hut (Dordrecht: Reidel), 161
- Gnedin, O. Y., Hernquist, L., & Ostriker, J. P. 1999, *ApJ*, 514, in press; [astro-ph/9709161](#)
- Gnedin, O. Y., & Ostriker, J. P. 1997, *ApJ*, 474, 223
- Gnedin, O. Y., & Ostriker, J. P. 1999, *ApJ*, 513, 626
- Goodman, J. 1987, *ApJ*, 313, 576
- Goodman, J. 1993, in *Structure and Dynamics of Globular Clusters*, *ASP Conf. Ser.*, vol. 50, ed. S. G. Djorgovski, & G. Meylan (San Francisco: ASP), 87
- Hénon, M. 1961, *Ann. d'Ap.*, 24, 369

- Johnston, K. V., Hernquist, L., & Weinberg, M. 1998, ApJ, submitted
- Kim, S. S., Lee, H. M., & Goodman, J., 1998, ApJ, 495, 786
- King, I. R. 1966, AJ, 71, 64
- Kundić, T., & Ostriker, J. P., 1994, ApJ, 438, 702
- Lee, H. M., 1987, ApJ, 319, 801.
- Lee, H. M., & Goodman, J. 1995, ApJ, 443, 109
- Lee, H. M., & Ostriker, J. P. 1987, ApJ, 322, 123
- Lee, H. M., & Ostriker, J. P. 1993, ApJ, 409, 617
- Lee, H. M., Fahlman, G. G., & Richer, H. B. 1991, ApJ, 366, 455
- Lynden-Bell, D. & Wood, R., 1968, MNRAS, 138, 495.
- Meylan, G., & Heggie, D. C. 1997, A&A Rev., 8, 1
- Murali, C., & Weinberg, M. D. 1997a, MNRAS, 288, 749
- Murali, C., & Weinberg, M. D. 1997b, MNRAS, 288, 767
- Murali, C., & Weinberg, M. D. 1997c, MNRAS, 291, 717
- Odenkirchen, M., Brosche, P., Geffert, M., & Tucholke, H.-J. 1997, New Astronomy, 2, 477
- Oh, K. S., & Lin, D. N. C., 1992, ApJ, 386, 519.
- Ostriker, J. P. 1985, in Dynamics of Star Clusters, IAU Symposium 113, ed. J. Goodman, & P. Hut (Dordrecht: Reidel), 347
- Ostriker, J. P., & Gnedin, O. Y. 1997, ApJ, 487, 667
- Ostriker, J. P., Spitzer, L. Jr., & Chevalier, R. A. 1972, ApJ, 176, L51
- Quinlan, G. D. 1996, New Astronomy, 1, 255
- Spitzer, L. Jr. 1940, MNRAS, 100, 397
- Spitzer, L. Jr. 1987, Dynamical Evolution of Globular Clusters (Princeton: Princeton University Press)
- Spitzer, L. Jr., & Chevalier, R. A. 1973, ApJ, 183, 565
- Spitzer, L. Jr., & Hart, M. H. 1971, ApJ, 164, 399
- Takahashi, K., 1995, PASJ, 47, 561
- Takahashi, K., 1997, PASJ, 49, 547
- Takahashi, K., Lee, H. M., & Inagaki, S. 1997, MNRAS, 292, 331
- Takahashi, K., & Portegies Zwart, S. F. 1998, ApJ, 503, L49
- Weinberg, M. D., 1994, AJ, 108, 1403

Table 1. Model parameters for NGC 6254.

Model	$c$	$t_{rh,0}$ (Gyr)	$t_{sh}/t_{rh,0}$	$t_{cc}/t_{rh,0}$	$t_d/t_{rh,0}$
SINGLE MASS	1.4	0.76	96		
<i>case 0</i>				12.9	32
<i>case 1</i>				10.0	26
<i>case 2</i>				11.2	32
<i>case 3</i>				9.7	24
LOW CONCENTRATION	0.84	1.80	7.3		
<i>case 0</i>				12.2	16.5
<i>case 1</i>				8.0	13.5
<i>case 2</i>				8.5	14.5
<i>case 3</i>				7.1	12
MULTI-MASS	1.4	2.77	15		
<i>case 0</i>				1.76	13.5
<i>case 1</i>				1.59	9.5
<i>case 2</i>				1.60	13
<i>case 3</i>				1.57	8.5

Table 2. Fitting coefficients for  $t_{cc}$  and  $t_d$  versus  $c$ .

Function	$a_1$	$a_2$	$a_3$	$a_4$	$a_5$
$f_1(c)$	1.3162	-1.9809	3.2910	-1.8401	0.2987
$f_2(c)$	1.2897	-1.1223	1.9824	-0.8803	0.1104
$f_3(c)$	0.1286	0.3173	-0.6573	0.6367	-0.1319

Table 3. Fitting coefficients for  $t_{cc}$  versus  $\beta$ .

$c$	$b_1$	$b_2$	$b_3$	$b_4$
0.8	1.5029	0.5539	0.0185	0.4558
1.0	0.1174	1.4184	1.6004	0.4491
1.2	0.5124	0.8597	1.5189	0.3840
1.4	3.3268	0.4680	-1.0819	0.5281
1.6	2.9924	0.4613	-1.0366	0.5726
1.8	1.1447	0.3691	0.1791	0.3614
2.0	1.4912	0.2996	-0.7153	0.1606
2.2	0.8931	0.6518	-0.6721	0.2626
2.4	0.6413	0.5716	-0.9622	0.2167
2.6	0.9452	0.5916	-1.4586	0.2065

Table 4. Fitting coefficients for  $t_d$  versus  $\beta$ .

$c$	$d_1$	$d_2$	$d_3$
0.8	2.1942	1.0376	2.3645
1.0	0.1315	1.2982	0.2646
1.2	1.6051	1.1528	2.6816
1.4	45.420	1.0356	74.731
1.6	135.52	0.9993	300.84
1.8	188.62	0.9932	587.29
2.0	159.24	0.9675	788.60
2.2	83.444	0.9608	667.98
2.4	40.040	1.0309	520.84
2.6	42.112	1.1056	862.75

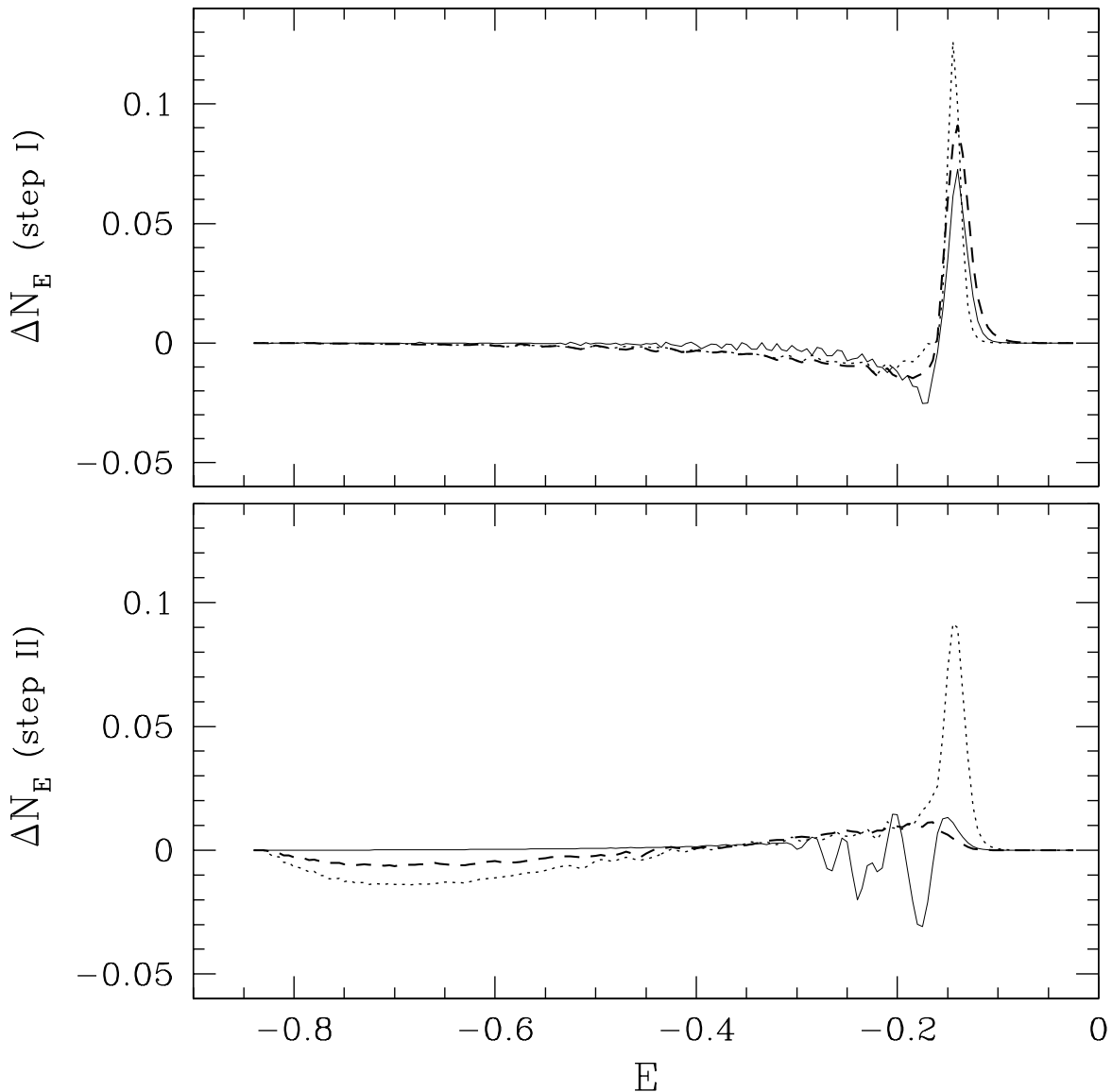


Fig. 1.— Comparison of the change of the energy density,  $\Delta N(E)$ , for the current Fokker-Planck models (*dashes*) and the  $N$ -body calculations (*solid lines*). Energy on the horizontal axis is normalized to the cluster binding energy. The test cluster is initially a King model with the concentration  $c = 0.84$ . A single weak shock is applied, similar to the ones studied by Gnedin & Ostriker (1999). *Top panel*: the energy change due to the shock; *Bottom panel*: the energy change due to the potential readjustment. Dots show previous implementation of tidal shocks in the F-P code, where the distribution function was kept fixed as a function of adiabatic invariants. The current procedure agrees with the  $N$ -body results more accurately, especially in the center and in the outer parts of the cluster.

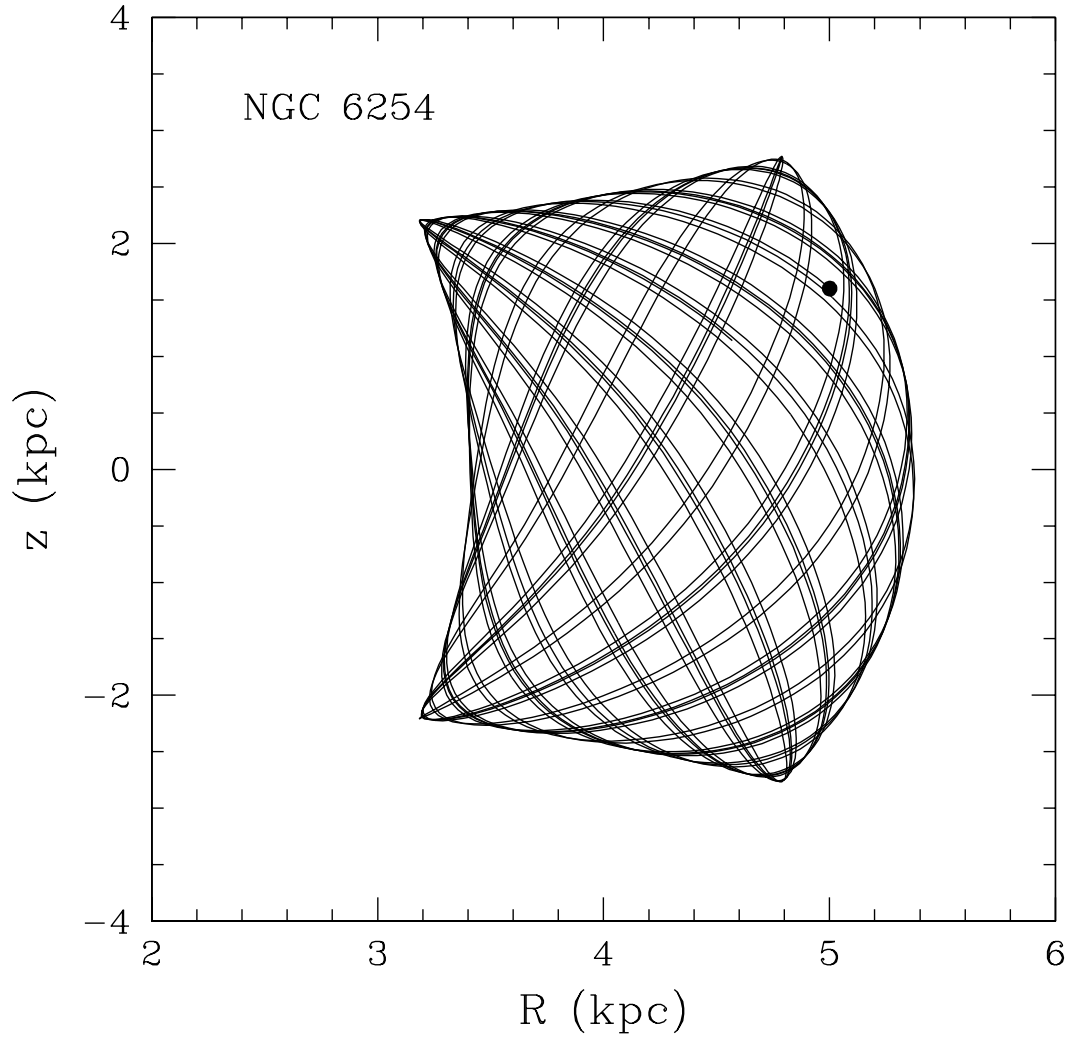


Fig. 2.— Orbits of NGC 6254 in the analytic potential of the Galaxy from Allen & Santillan (1991), for a period of  $3 \times 10^9$  years. The dot marks the current position of the cluster.

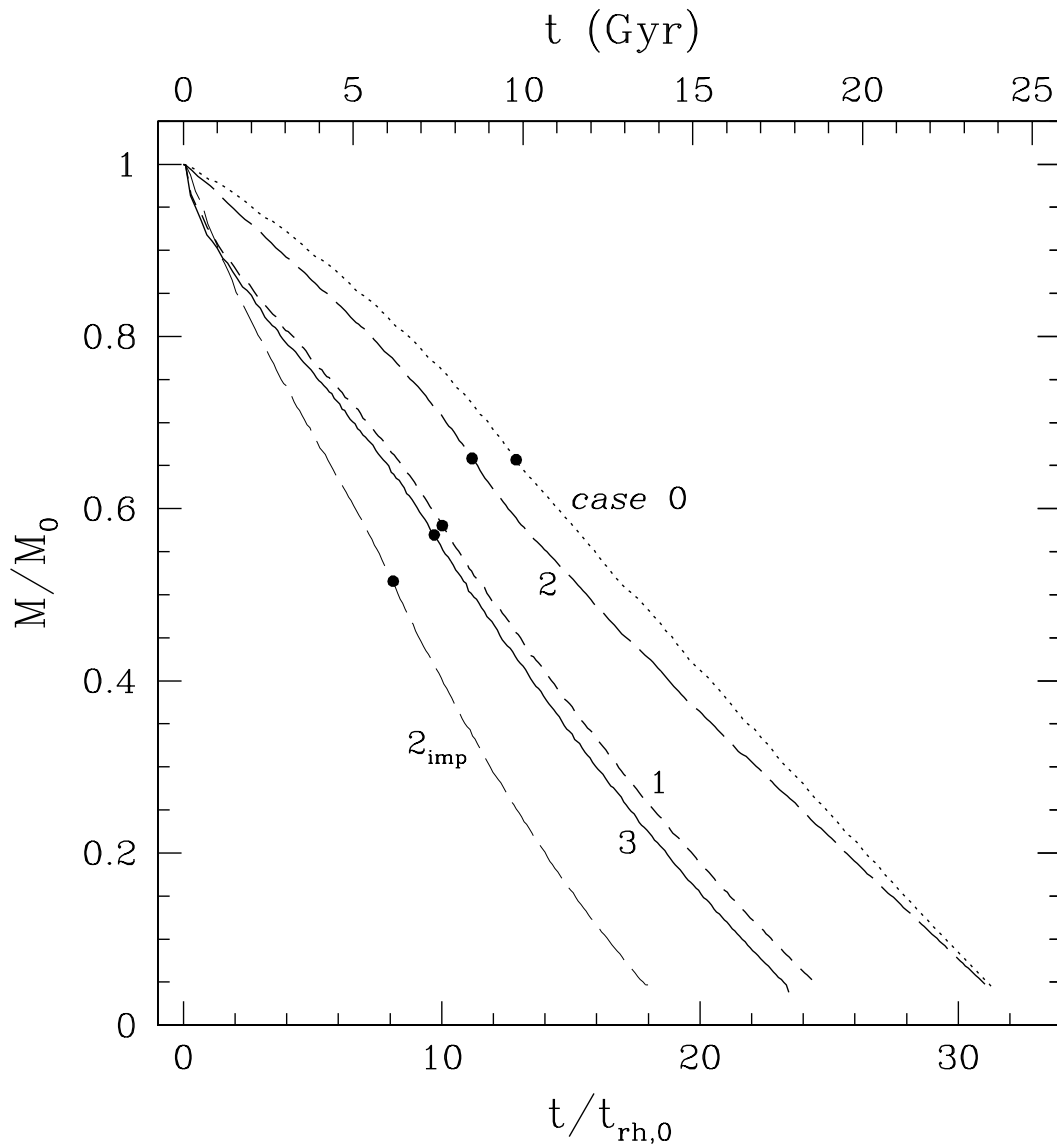


Fig. 3.— The mass loss for the single-mass models of globular cluster NGC 6254. Time is expressed in units of the initial half-mass relaxation time, as well as in billions of years. Dots are for the model with two-body relaxation only (*case 0*), dashes are for the model that includes the effects of the energy shift due to tidal shocks (*case 1*), long dashes are for the model that includes the second order energy dispersion (without the heating term; *case 2*), and the solid line is for the final model including proper treatment of all of the shock effects (*case 3*). The adiabatic corrections for “slow shocks” are used (eq. [7]). For illustration, thin dashes show the effect of the second order term (marked “ $2_{imp}$ ”) if it had not had adiabatic corrections. Filled circles indicate the time of maximum core collapse.

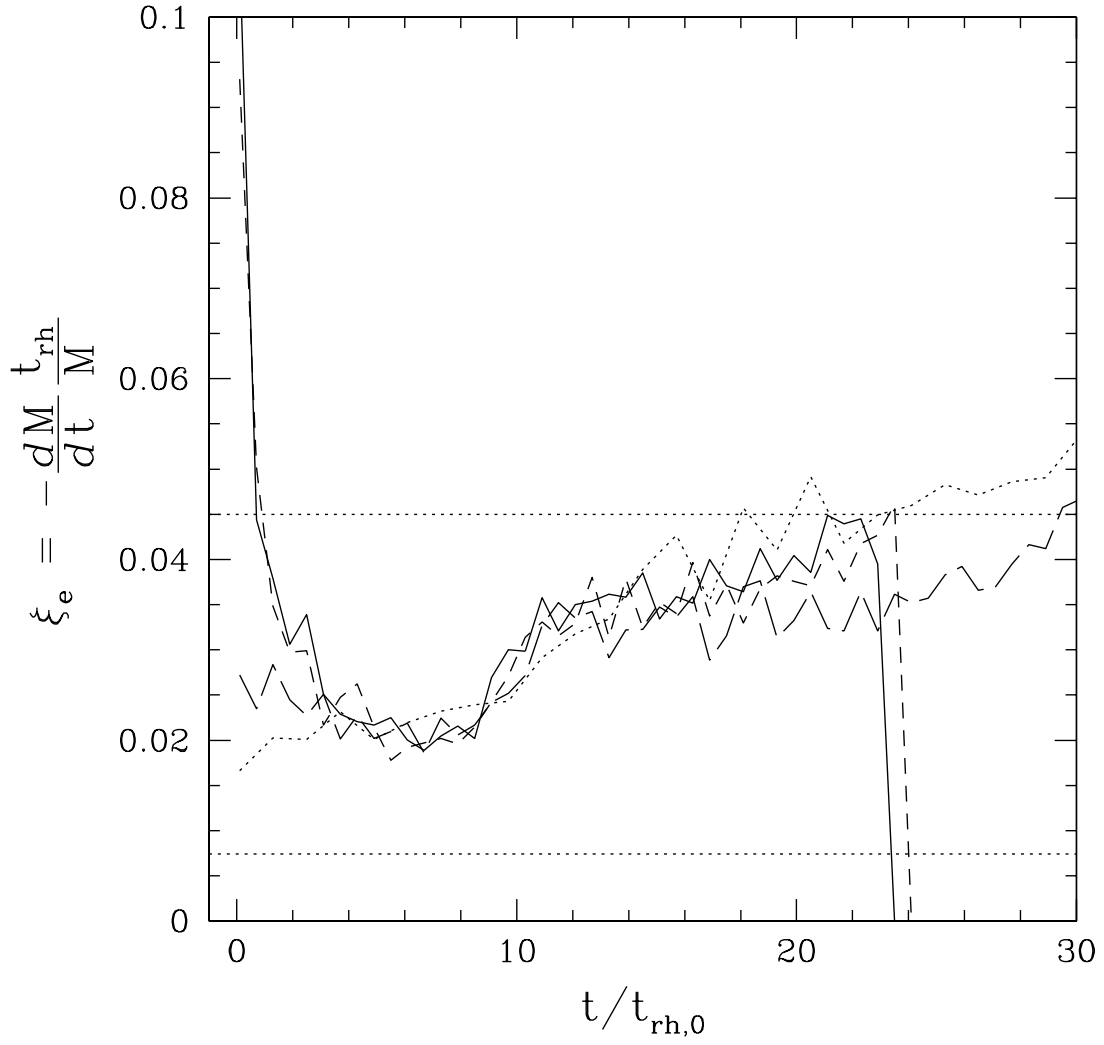


Fig. 4.— Escape probability in units of the half-mass relaxation time for NGC 6254. Line notation is the same as in Fig. 3. The lower horizontal line shows the analytical estimate by Ambartsumian (1938),  $\xi_e = 0.0074$ , and the upper self-similar calculations by Hénon (1961),  $\xi_e = 0.045$ .



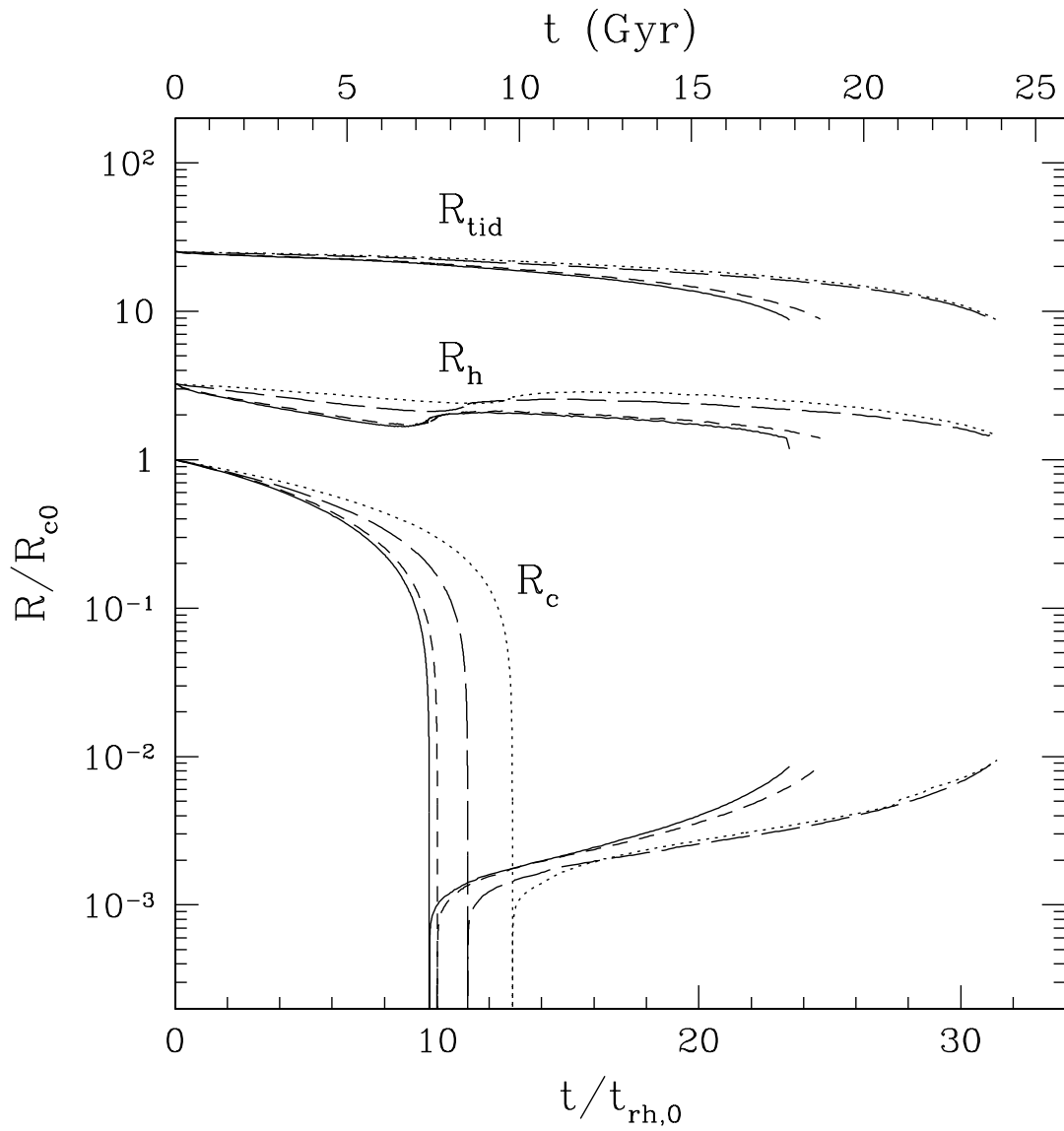


Fig. 5.— Evolution of the tidal, half-mass, and core radii of NGC 6254. Line notation is the same as in Fig. 3.

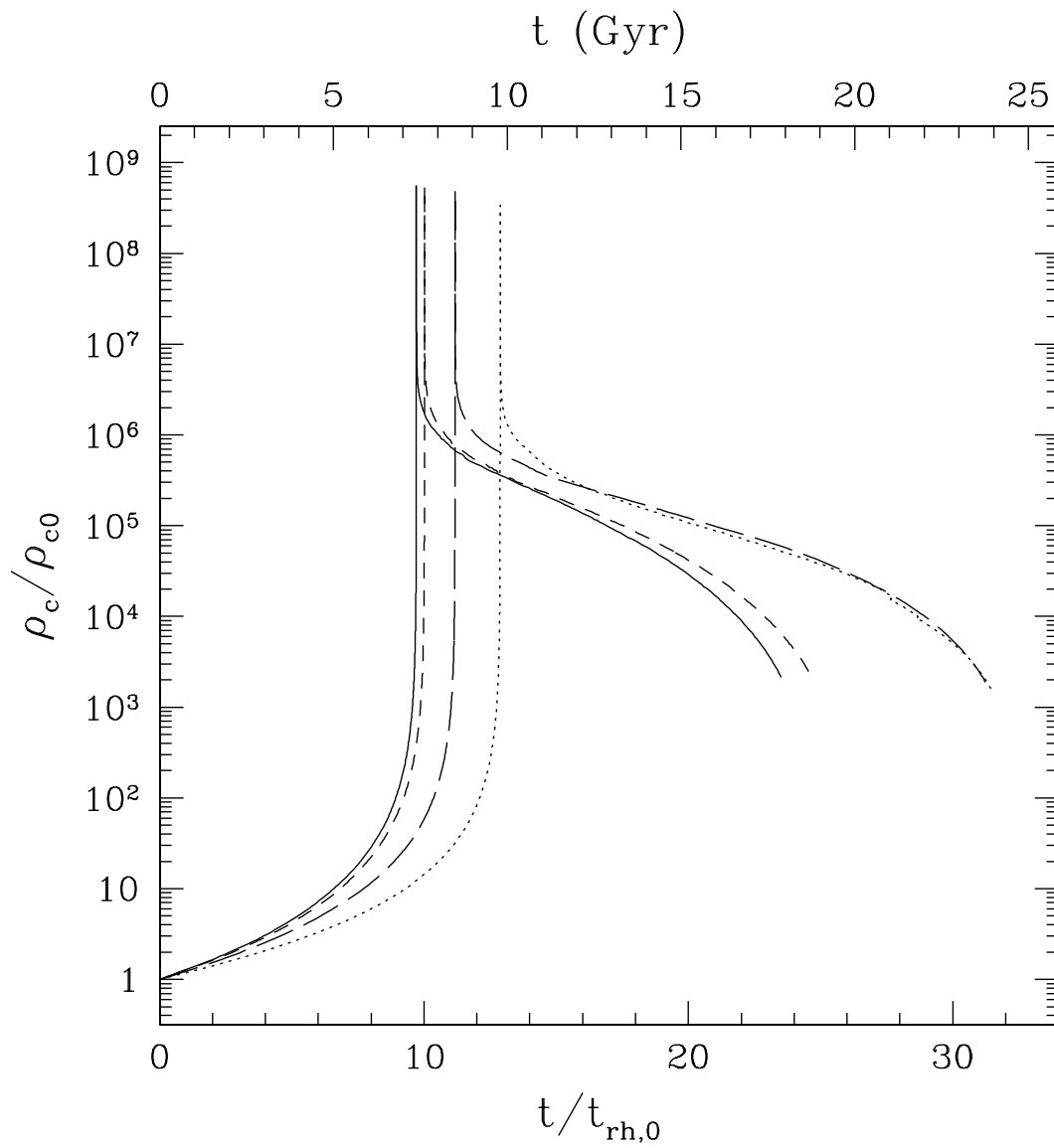


Fig. 6.— Evolution of the central density of NGC 6254. Line notation is the same as in Fig. 3.

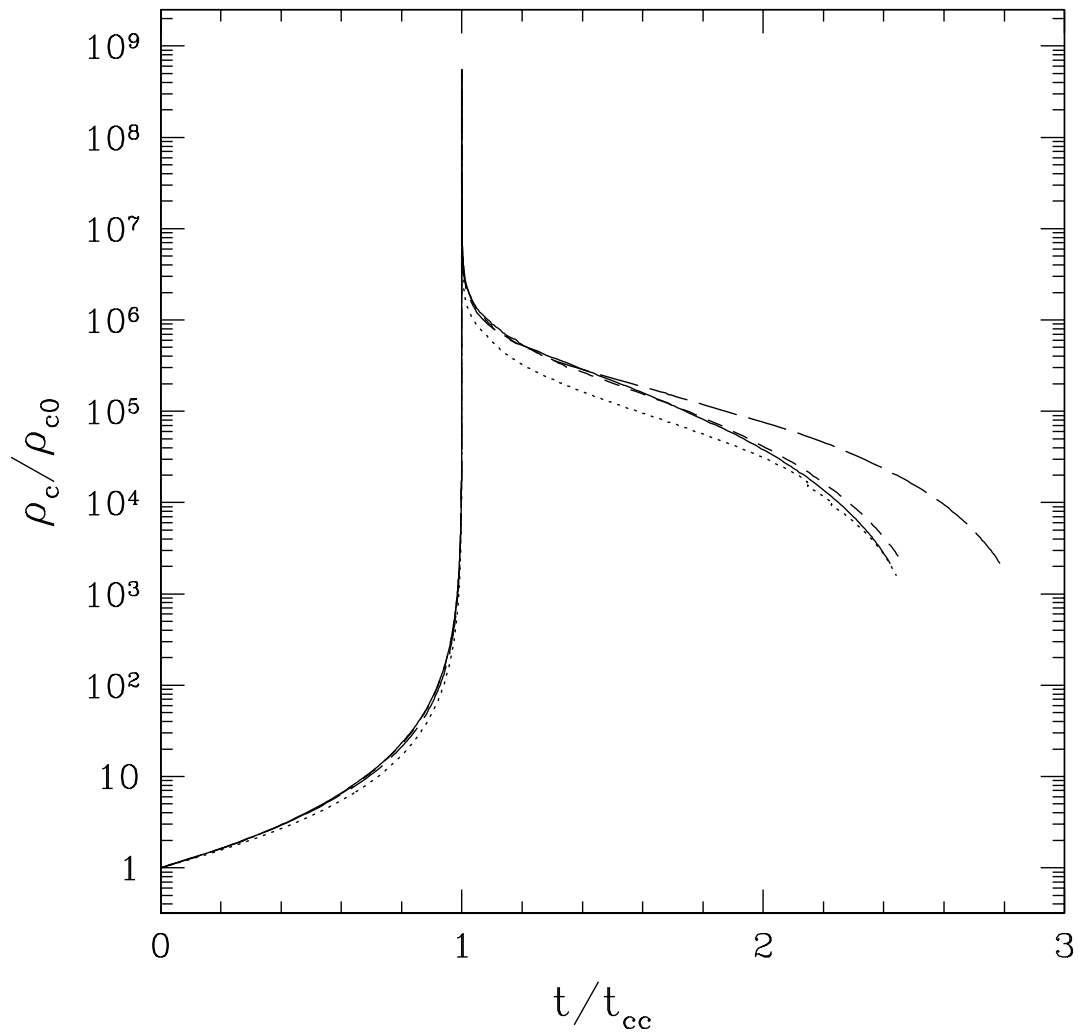


Fig. 7.— Central density of NGC 6254 vs. time scaled to the individual core collapse times. Evolution in these scaled units is similar for all models. Line notation is the same as in Fig. 3.

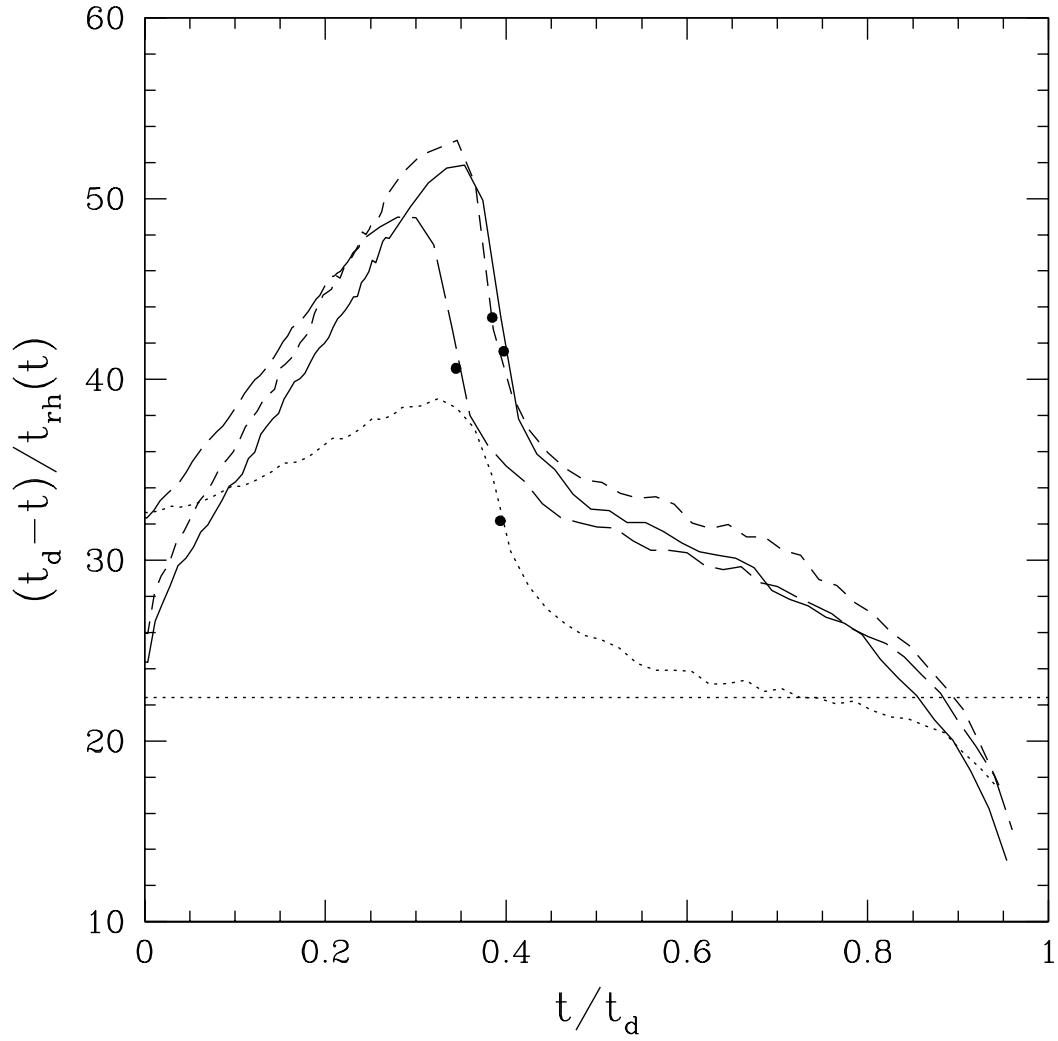


Fig. 8.— Time to destruction of the cluster NGC 6254 in units of the current relaxation time,  $t_{rh}(t)$ , vs. cluster age. Line notation is the same as in Fig. 3. The filled circles indicate the time of maximum core collapse. The dotted horizontal line is Hénon’s self-similar solution, equation (23). The abscissa is normalized to the different destruction time  $t_d$  for each model.

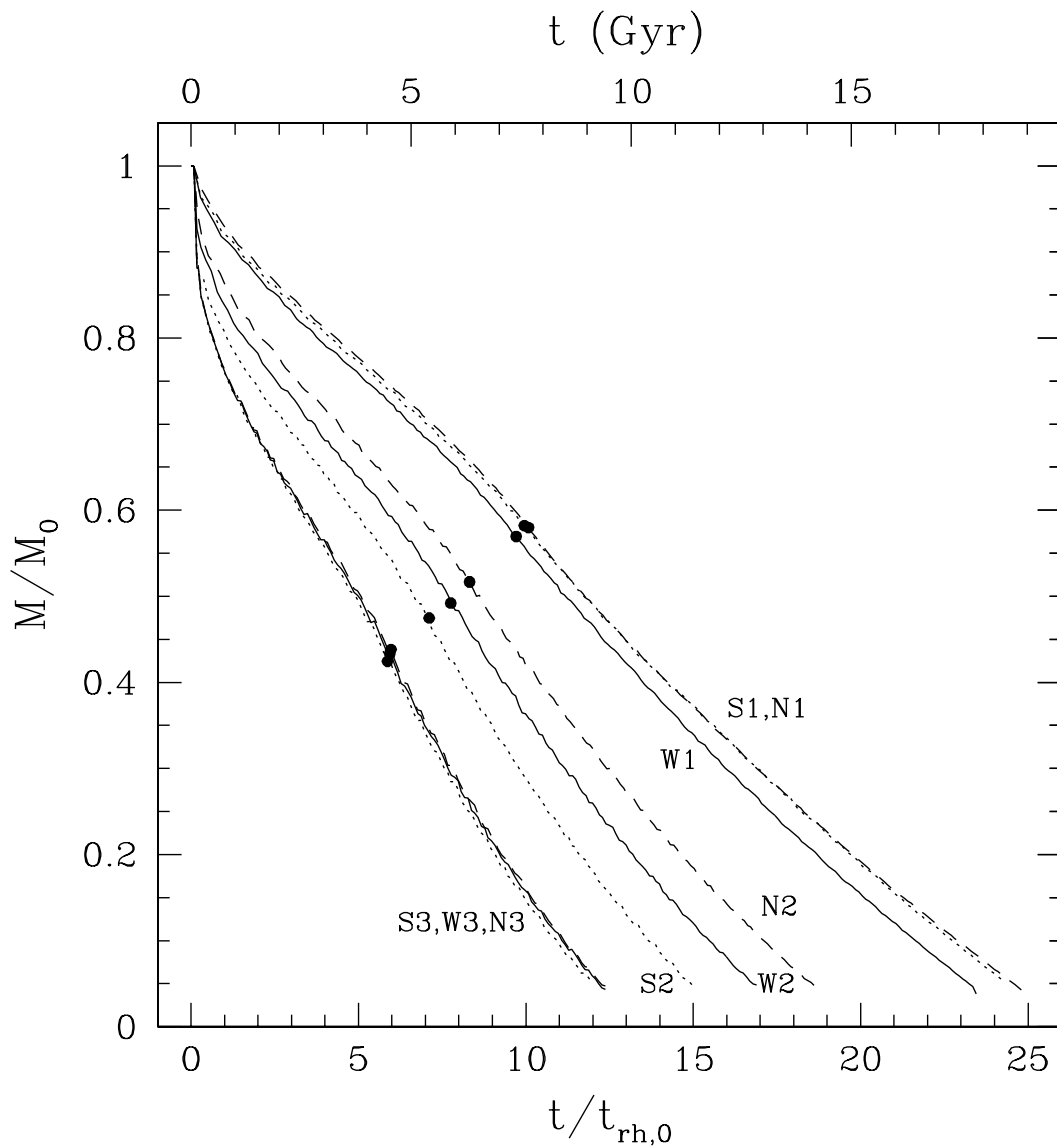


Fig. 9.— Comparison of the Spitzer ( $S$ ), Weinberg ( $W$ ), and  $N$ -body ( $N$ ) adiabatic corrections for the *case 3* models of NGC 6254. The first set of models ( $S1, W1, N1$ ) is calculated with the true values of the disk and bulge shock timescales,  $\tau_{\text{disk}}$  and  $\tau_{\text{bulge}}$ ; the second set ( $S2, W2, N2$ ) with the shock timescales reduced by a factor of 5; and the third set ( $S3, W3, N3$ ) with the shock timescales reduced by a factor of 100. Solid lines correspond to the Weinberg corrections (eq. [7]), dots to the Spitzer corrections (eq. [6]), and dashes to the  $N$ -body corrections for fast shocks (eq. [8]). Filled circles indicate the time of maximum core collapse.

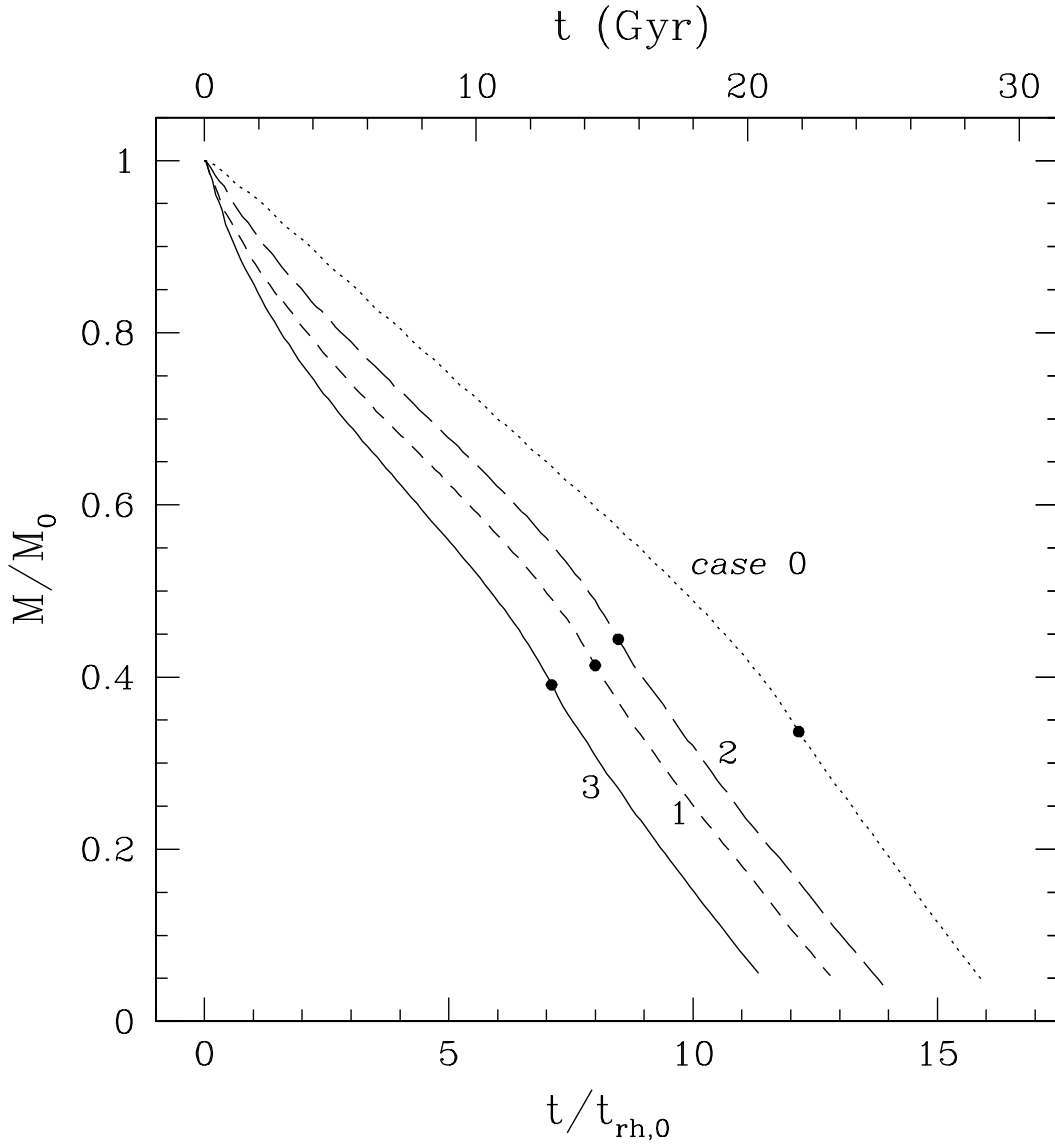


Fig. 10.— The mass loss of the low concentration model,  $c=0.84$ . All other parameters of NGC 6254 are fixed, including the tidal radius in parsecs. Line notation is the same as in Fig. 3.

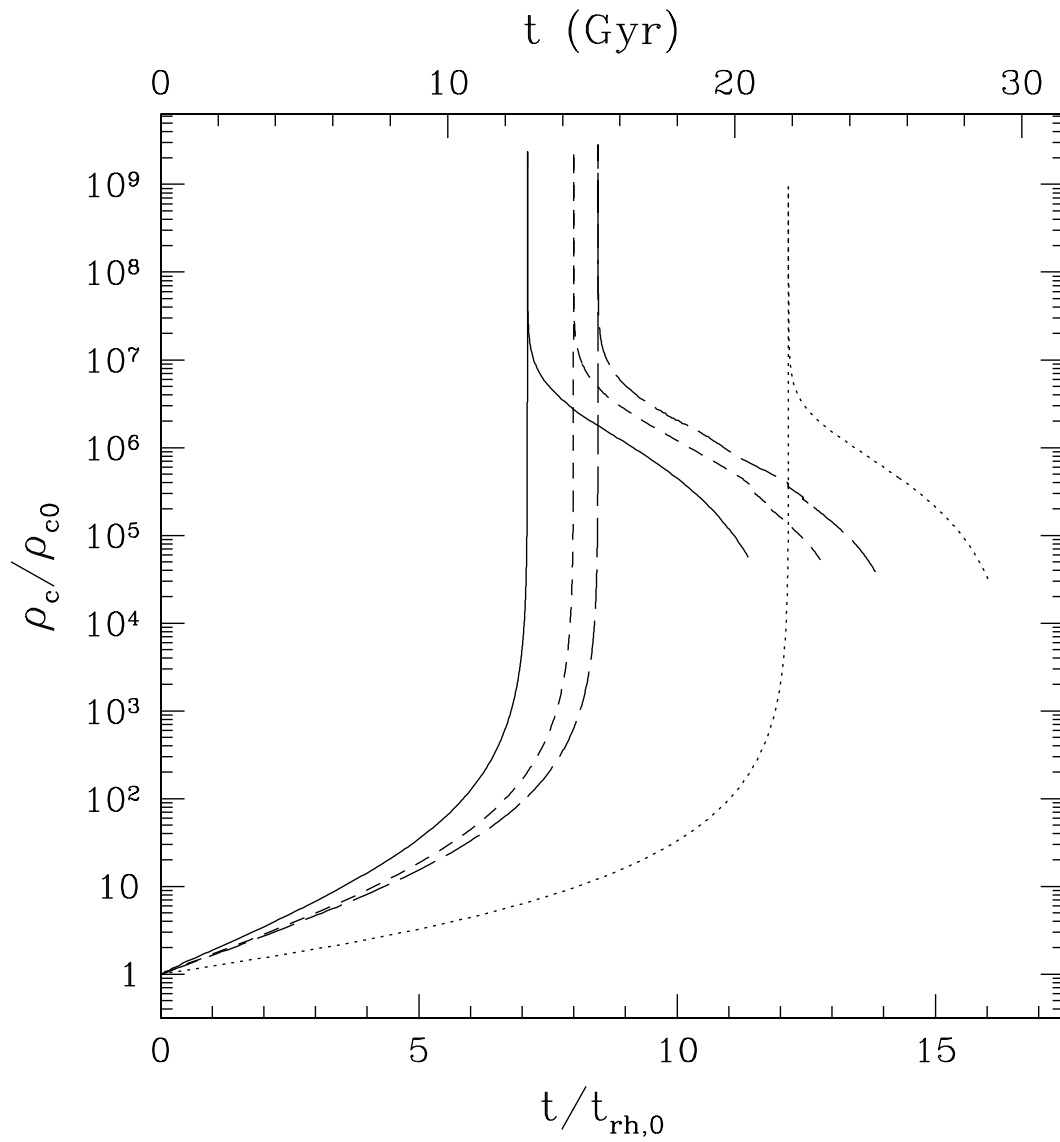


Fig. 11.— Central density of the low concentration cluster. Line notation is the same as in Fig. 3.

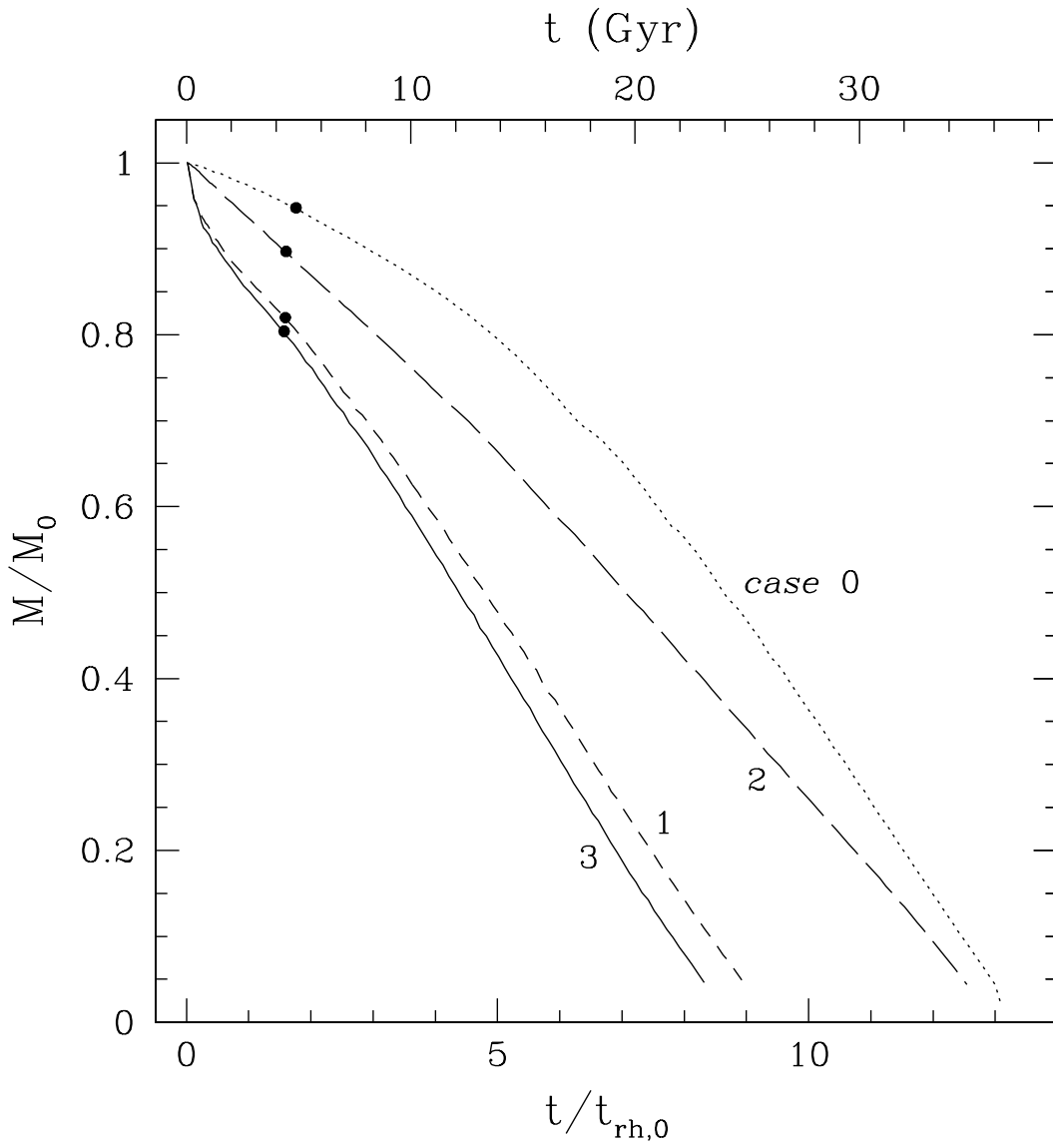


Fig. 12.— The mass loss of the multi-mass model of NGC 6254. Line notation is the same as in Fig. 3.



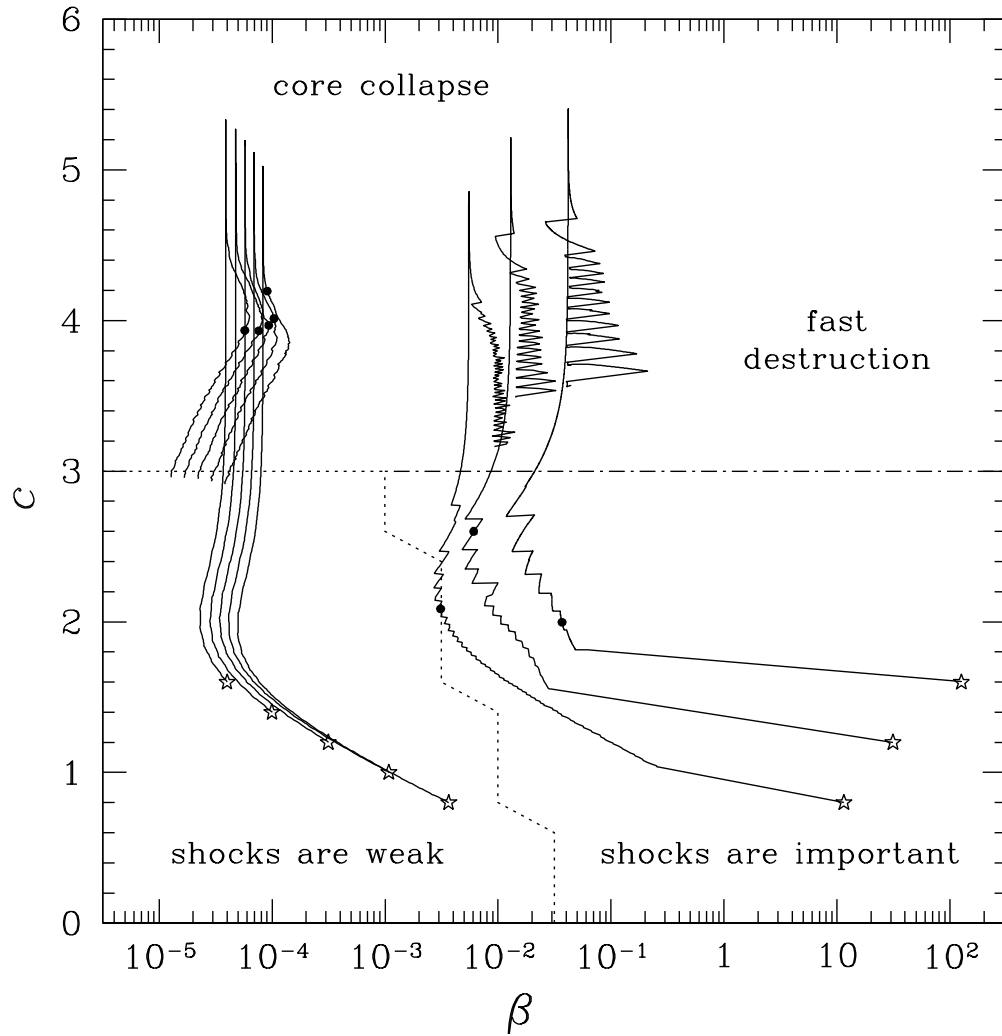


Fig. 13.— Evolution of the model clusters as a function of the concentration,  $c$ , and the shock parameter,  $\beta$ . Stars show the initial conditions, filled circles the time of core collapse. Marked regions on the diagram correspond to the different regimes of cluster evolution. The critical values of  $\beta$ , separating the left and right regions, are determined when the core collapse time deviates from its value for  $\beta = 0$ .

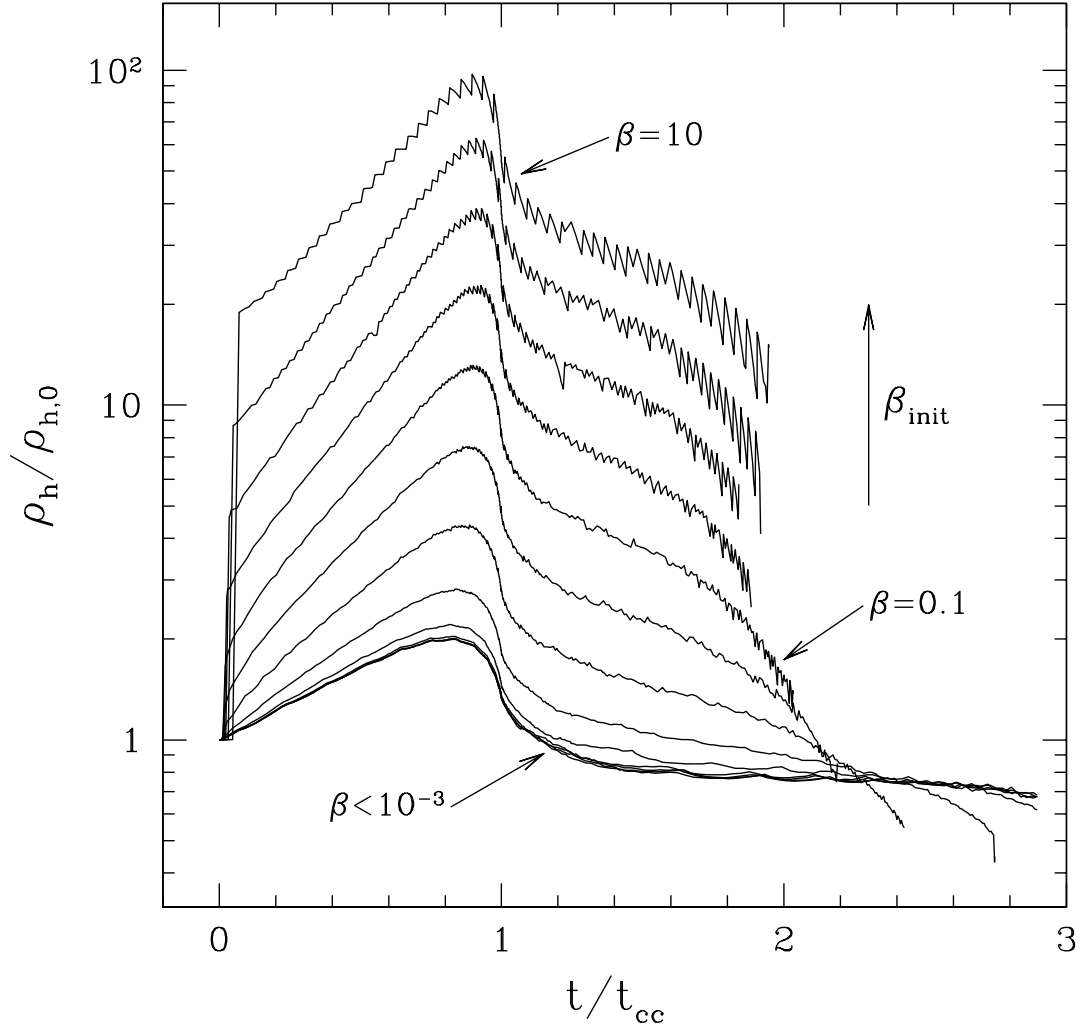


Fig. 14.— The mean density,  $\rho_h$ , as a function of time normalized to the individual core collapse time for each run. All models shown have the same initial concentration  $c = 1.4$  but different shock parameters varying from  $\beta = 10^{-5}$  to  $\beta = 10$ . Models with  $\beta < 10^{-3}$  show essentially identical evolution. At the time of core collapse, the mean density is higher for the higher values of  $\beta$ .

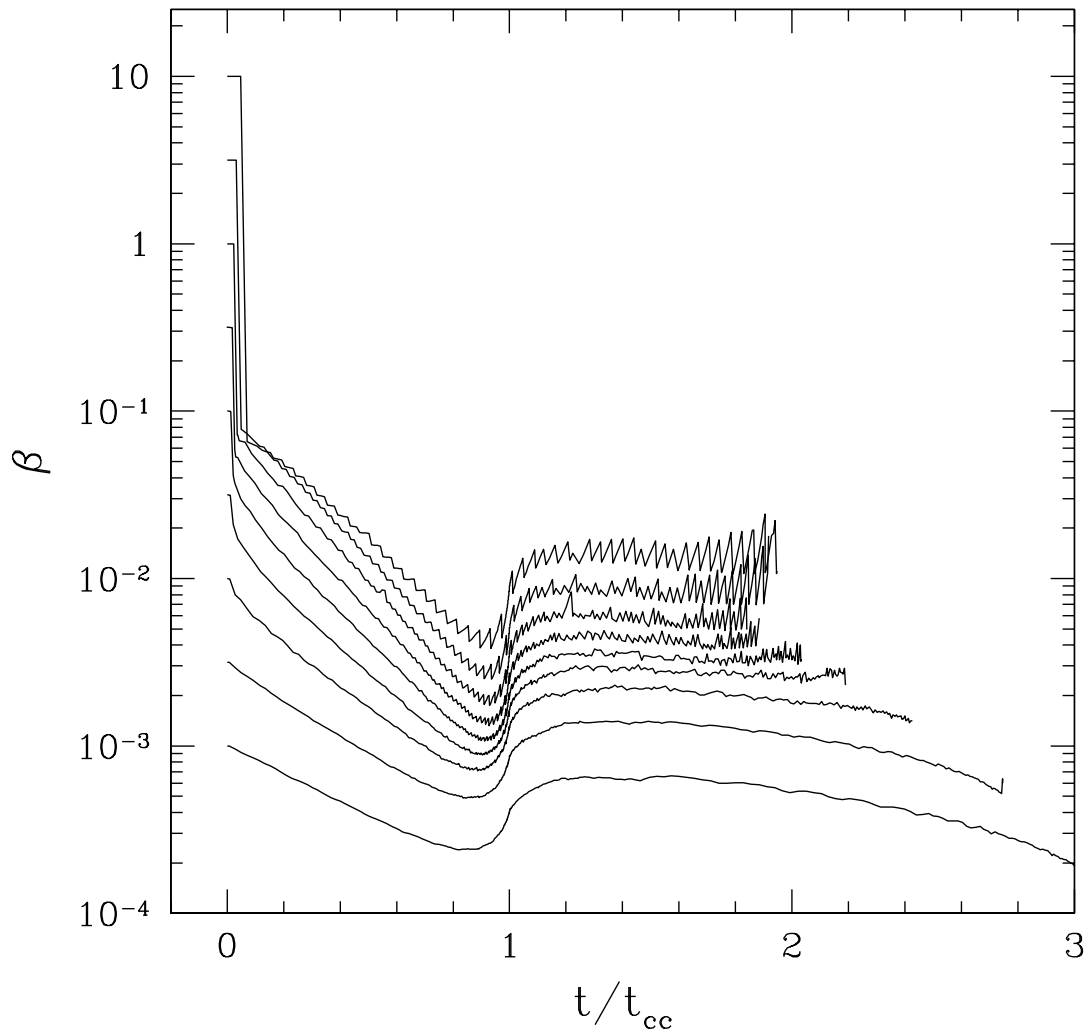


Fig. 15.— The shock parameter,  $\beta$ , as a function of time normalized to the individual core collapse time, for the models with the various initial values of  $\beta$  and the same initial concentration  $c = 1.4$ .

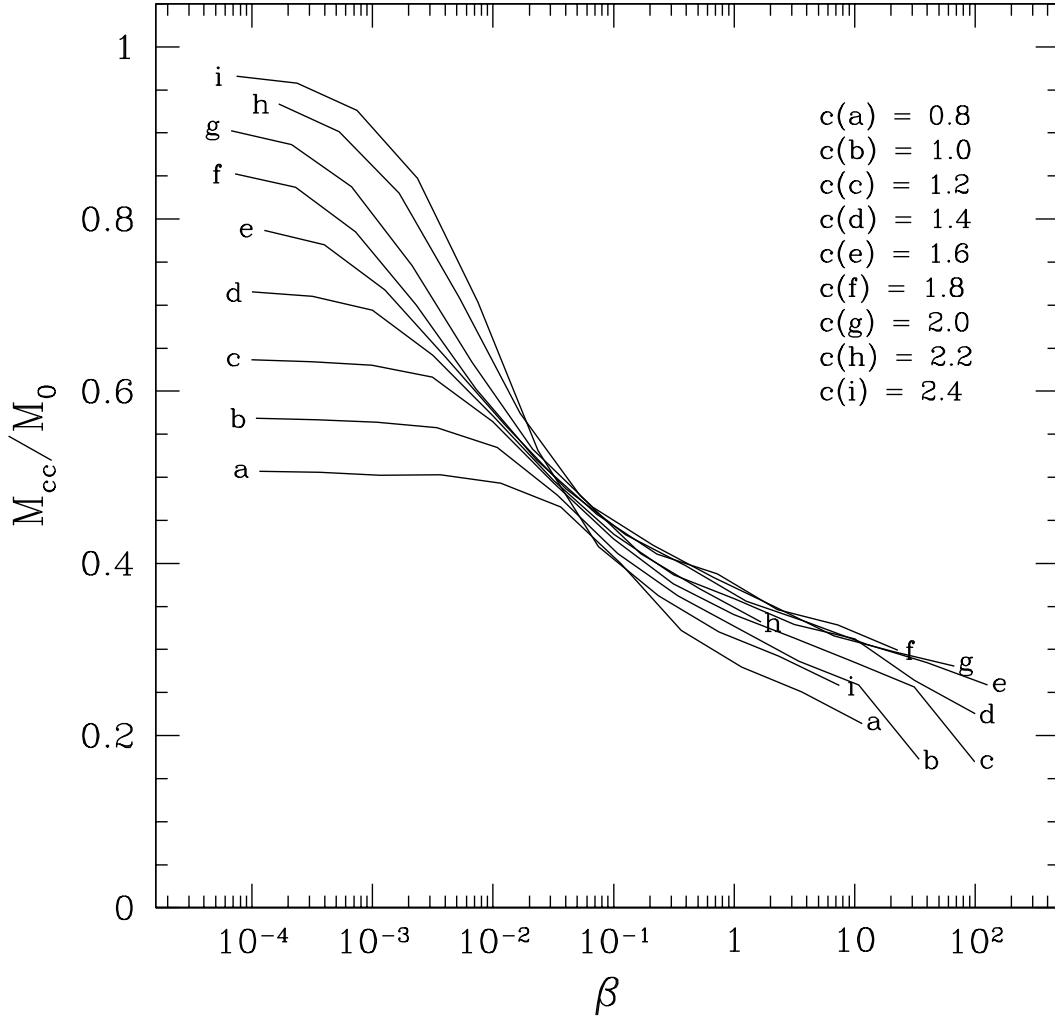


Fig. 16.— The mass remaining at the time of core collapse vs. the shock parameter,  $\beta$ , for the various families of cluster models. Each family has the same initial concentration, from  $c = 0.8$  for family  $a$  to  $c = 2.4$  for family  $i$ . Letters correspond to the end models of each family.

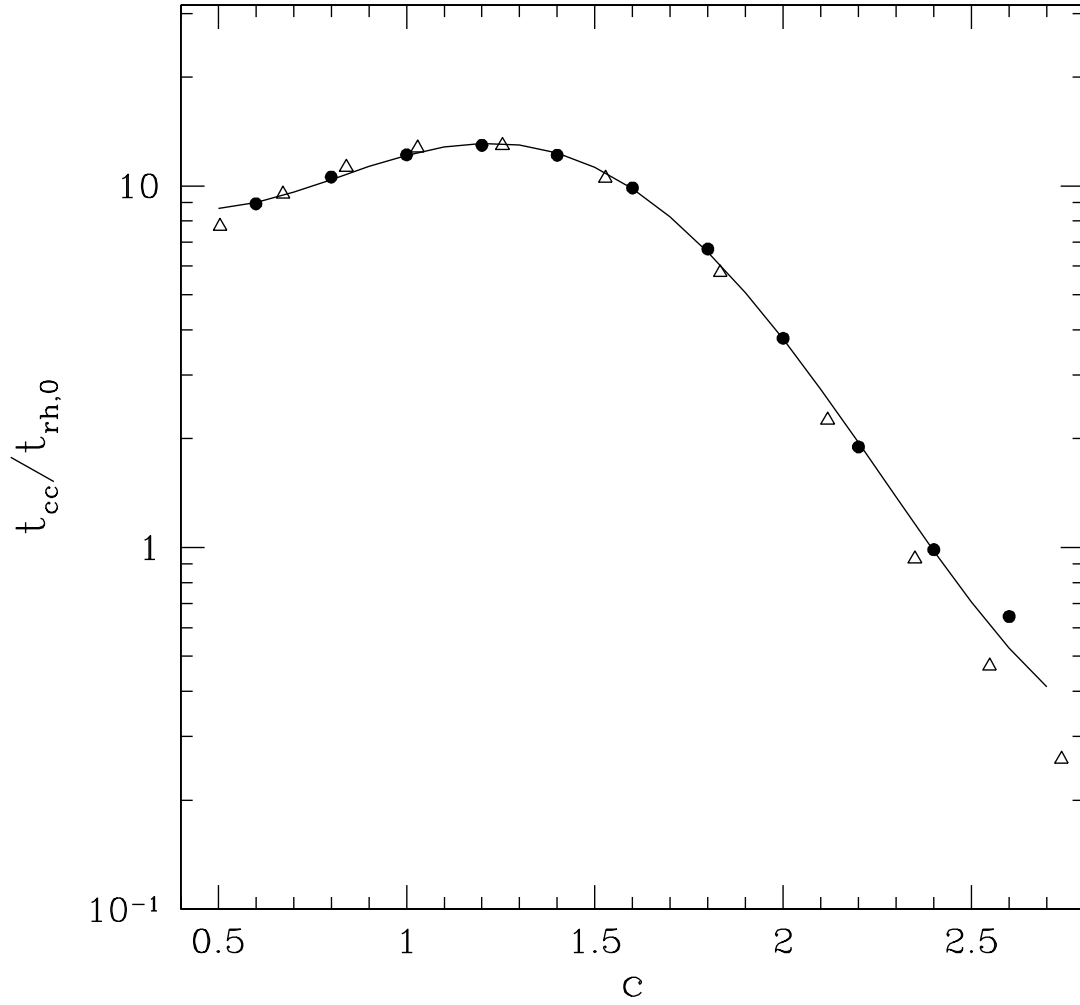


Fig. 17.— The core collapse time as a function of the initial concentration for the models without tidal shocks. Filled dots are our results, triangles are from Quinlan (1996). The agreement is very good, except for the very high concentration clusters. The solid line is our fit, eq. (27), with the last point excluded.

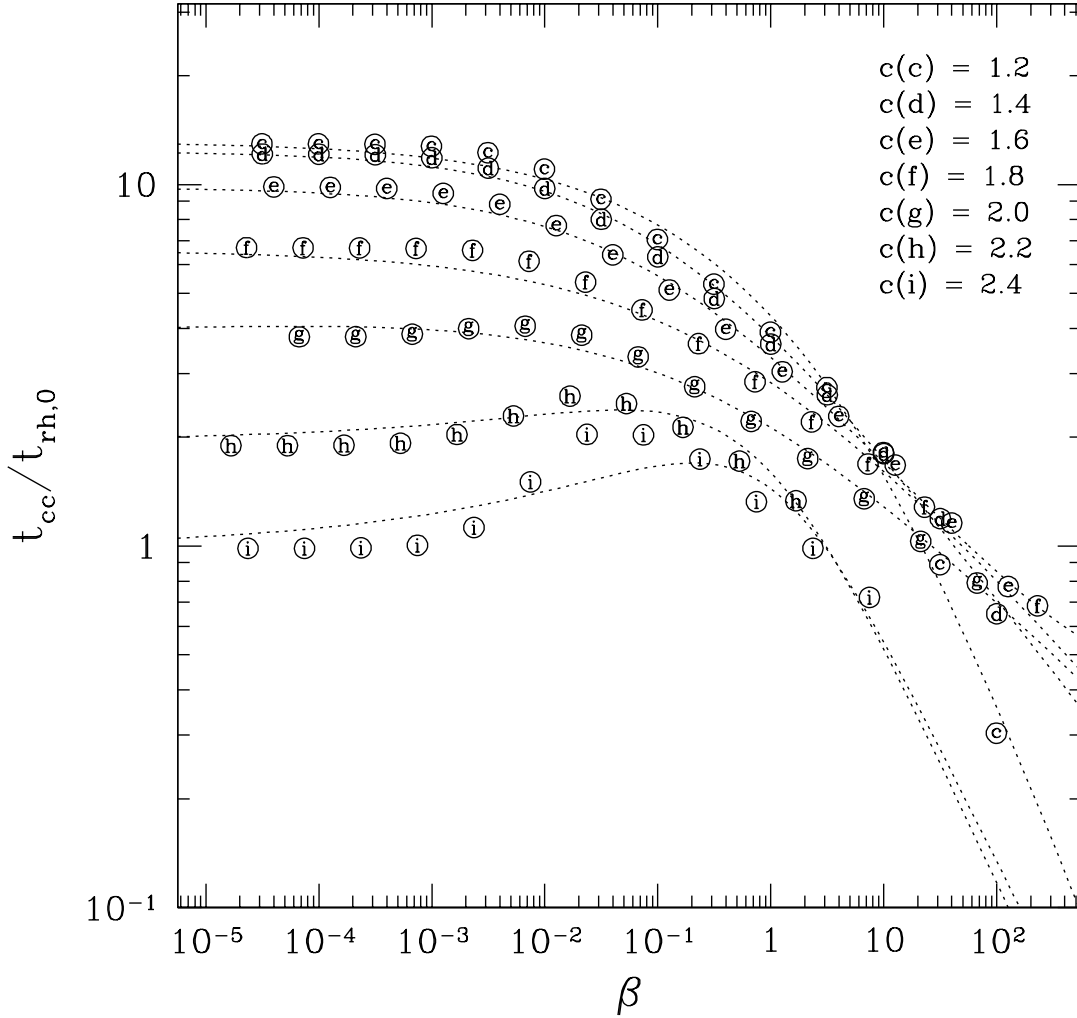


Fig. 18.— The core collapse time as a function of the shock parameter,  $\beta$ . The families of models with the initial concentrations  $c = 0.8$  (a) and  $c = 1.0$  (b) are excluded for clarity. Dotted lines are our fit, eq. (28).

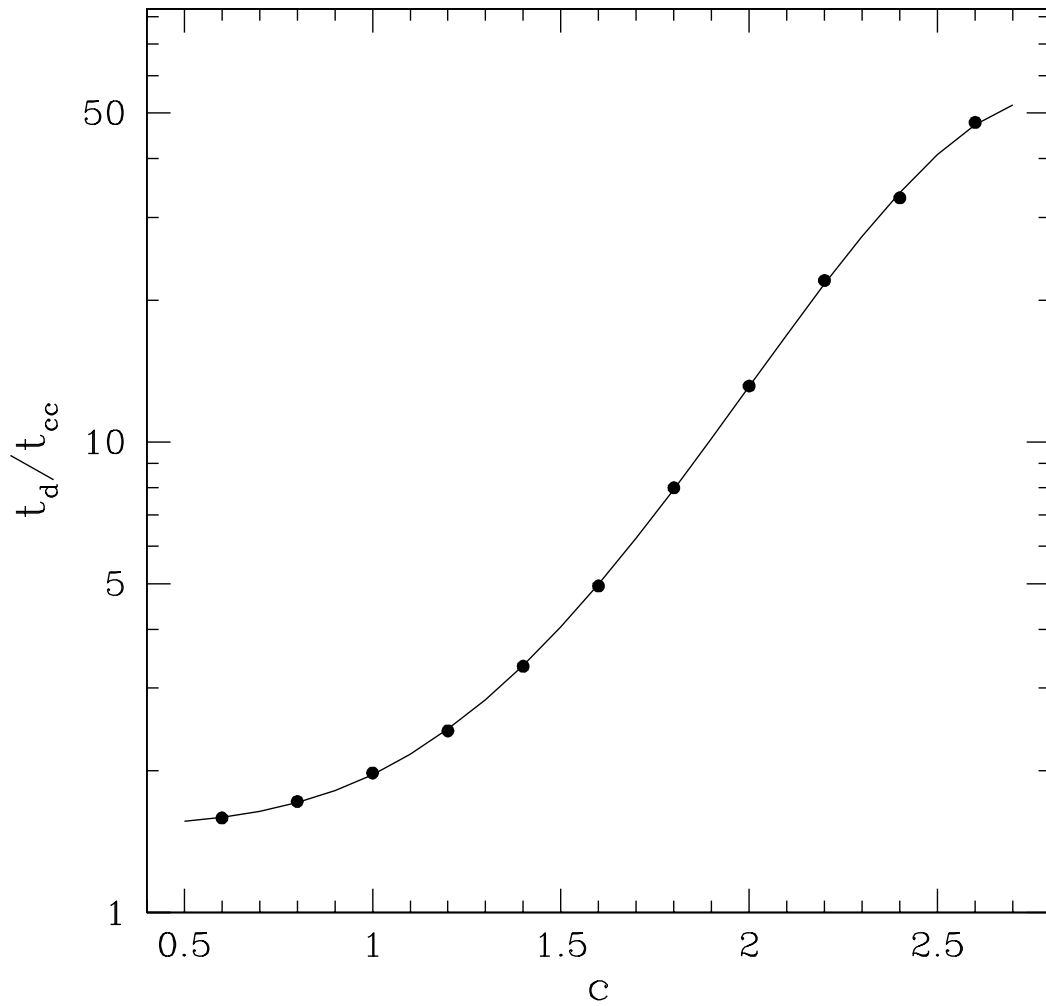


Fig. 19.— The destruction time in units of the core collapse time vs. cluster concentration for the models without tidal shocks. The solid line is our fit, eq. (29).

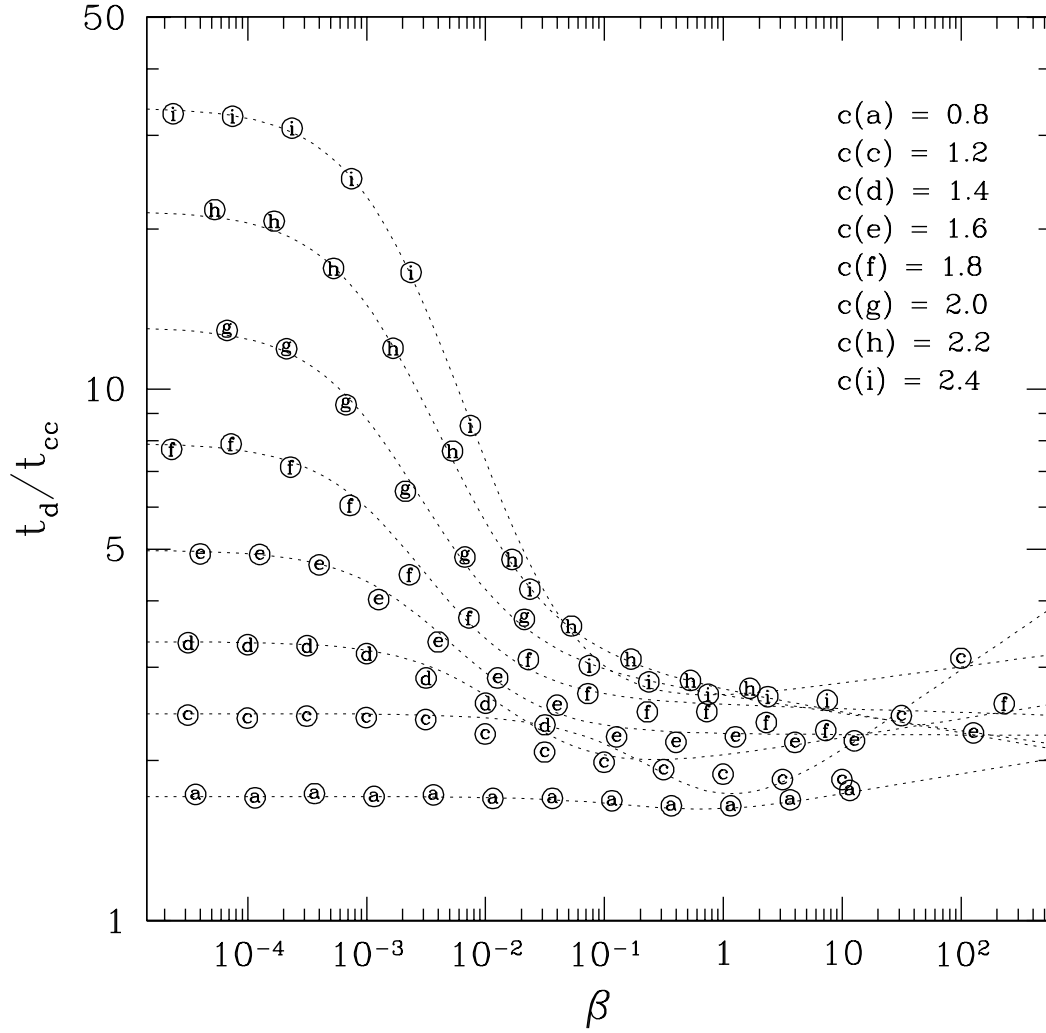


Fig. 20.— The destruction time as a function of the shock parameter,  $\beta$ . For clarity, some of the models are shown only for  $\beta \lesssim 0.03$ . Dotted lines are our fit, eq. (30).